

What do larger image classifiers memorise?

Michal Lukasik
mlukasik@google.com

Vaishnavh Nagarajan
vaishnavh@google.com

Ankit Singh Rawat
ankitsrawat@google.com

Aditya Krishna Menon
adityakmenon@google.com

Sanjiv Kumar
sanjivk@google.com

Google Research, New York

Abstract

The success of modern neural networks has prompted study of the connection between *memorisation* and *generalisation*: overparameterised models generalise well, despite being able to perfectly fit (“memorise”) completely random labels. To carefully study this issue, Feldman [29] proposed a metric to quantify the degree of memorisation of individual training examples, and empirically computed the corresponding memorisation profile of a ResNet on image classification benchmarks. While an exciting first glimpse into what real-world models memorise, this leaves open a fundamental question: *do larger neural models memorise more?* We present a comprehensive empirical analysis of this question on image classification benchmarks. We find that training examples exhibit an unexpectedly diverse set of memorisation trajectories across model sizes: most samples experience *decreased* memorisation under larger models, while the rest exhibit *cap-shaped* or *increasing* memorisation. We show that various proxies for the Feldman [29] memorization score fail to capture these fundamental trends. Lastly, we find that knowledge distillation — an effective and popular model compression technique — tends to inhibit memorisation, while also improving generalisation. Specifically, memorisation is mostly inhibited on examples with increasing memorisation trajectories, thus pointing at how distillation improves generalisation.

1 Introduction

Statistical learning is conventionally thought to involve a delicate balance between *memorisation* of training samples, and *generalisation* to test samples [36]. However, the success of *overparameterised* neural models challenges this view: such models generalise well, despite having the capacity to memorise, e.g., by perfectly fitting completely random labels [83]. Indeed, in practice, such models typically *interpolate* the training set, i.e., achieve zero misclassification error. This has prompted a series of analyses aiming to understand why such models can generalise [7, 16, 9, 61, 8, 77].

Recently, Feldman [29] established that in some settings, memorisation may be *necessary* for generalisation. Here, “memorisation” is defined via a theoretically-grounded stability-based notion, where the high memorisation examples are the ones that the model can correctly classify only if they are present in the training set (see Equation 1 in §2). This definition allows the level of memorisation¹ of a training sample to be *estimated* for real-world neural models. To that end, Feldman and Zhang [30] studied the memorisation profile of a ResNet on standard image classification benchmarks.

¹From hereon in, unless otherwise noted, we shall use “memorisation” to refer to the stability-based notion of Feldman [29]; see Equation 1.

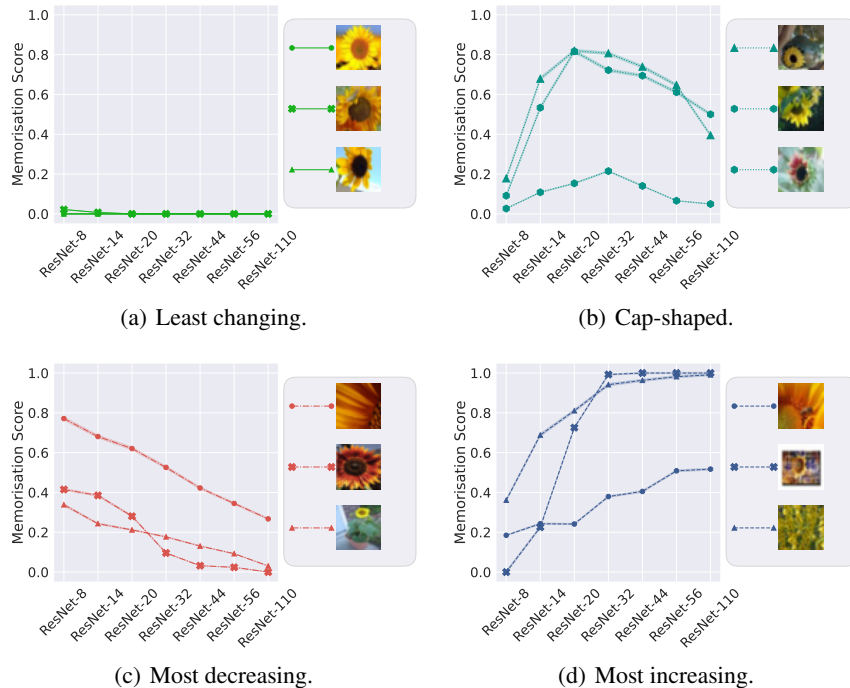


Figure 1: Training examples on CIFAR-100 exhibit a diverse set of memorisation trajectories across model depths: fixing attention on training examples belonging to the sunflower class, while many examples unsurprisingly have fixed, decreasing or cap-shaped memorisation scores (green, red and teal curves), there are also examples with increasing memorisation even after interpolation (blue curves). In §3.2 we discuss their characteristics in more detail, e.g. how these trajectories constitute a vast majority of trajectories seen in the data.

While an exciting first glimpse into how real-world models memorise, it does not tell us how memorisation varies with model size. After all, varying the model size is an important practical consideration: training models of different sizes within a single family (e.g., ResNet [39], MobileNet [44], and T5 [69]) is commonplace, as it enables practitioners to deploy the best performing models while respecting their computation budget for both training and inference. Is the improved performance realized by increasing model size merely a result of increased memorisation of training samples by the larger models, or their improved generalisation? While larger models have more capacity for memorisation, it is yet not well understood whether the result of the commonly used training recipes (e.g., based on SGD) indeed result in models that increasingly memorise more as the model size increases.

Practitioners also employ a systematic approach to obtain high quality models of varying size: knowledge distillation. In particular, it involves developing good-quality small (student) models by drawing supervision from high-performing large (teacher) models. Fundamentally, distillation involves interaction among models of different sizes, and thus a further question can be posed: how does the interaction between the teacher and the student impact the smaller model’s memorisation?

This paper conducts a systematic and comprehensive empirical study to answer the aforementioned questions. In particular, using the theoretically-grounded notion of memorisation from Feldman [29], we analyse the interplay between memorisation and generalisation across different model sizes. Based on our controlled experiments, we make the following contributions:

- (i) we present a quantitative analysis of how memorisation varies with model complexity (e.g., depth or width of a ResNet) for image classifiers. Our main findings are that increasing the model complexity tends to make the distribution of memorisation across examples more *bi-modal* (Section 3.3). At the same time, we identify that existing computationally-tractable alternatives of quantifying memorisation and example difficulty do not capture this key trend (Section 3.5).

- (ii) to further probe into the bi-modal memorisation trend, we present examples exhibiting varying memorisation score trajectories across model sizes, and identify four most prominent trajectory types, including those where memorisation *increases* with model complexity. We find that particularly *ambiguous and mislabeled* examples exhibit this kind of trajectory (Section 3.4).
- (iii) we conclude with a quantitative analysis demonstrating that distillation tends to inhibit memorisation, particularly of samples that the one-hot (i.e., non-distilled) student memorises. Intriguingly, we find that the memorisation is mostly inhibited on the examples for which memorisation increases as the model size increases. This observation leads to conclude that distillation improves generalisation by limiting memorisation of such hard examples (Section 4).

2 Background and related work

The term “memorisation” is often invoked when discussing supervised learning, but with several distinct meanings. A classical usage refers to models that simply construct a fixed *lookup table*, viz. a table mapping certain keys to targets (e.g., labels) [27, 22]. Noting that the 1-nearest neighbour algorithm can *interpolate* the training data (i.e., perfectly predict every training sample), some works instead use “memorisation” as a synonym for interpolation [83, 3, 73]. A more general definition is that “memorisation” occurs when the training error is lower than the best achievable error (or *Bayes-error*) [17, 23]. We summarise more notions of memorisation in Table 1 (Appendix).

While each of these notions imply “memorising” the *entire* training set, one may also ask whether a *specific* sample is memorised. One intuitive formalisation of this notion is that the model predictions change significantly when a sample is removed from training [29, 46], akin to algorithmic stability [13]. More precisely, consider a training sample S comprising N *i.i.d.* draws from some distribution D over labelled inputs $(x, y) \in \mathcal{X} \times \mathcal{Y}$. A learning *algorithm* is some randomised function $A(\cdot; S): \mathcal{X} \rightarrow \mathcal{Y}$, where the randomness is, e.g., owing to initialisation, ordering of mini-batches, and stochasticity in parameter updates. The *memorisation score* of a sample $(x, y) \in S$ is then [29]:

$$\text{mem}(x, y; S) = \underbrace{\mathbb{P}(y = A(x; S))}_{\text{in-sample acc.}} - \underbrace{\mathbb{P}(y = A(x; S - \{(x, y)\}))}_{\text{out-sample acc.}}. \quad (1)$$

Here, $\mathbb{P}(\cdot)$ considers the randomness in the learning algorithm. Intuitively, this is the excess classification accuracy on the sample (x, y) when it is *included* versus *excluded* in the training sample. Large neural models can typically drive the first term to 1 for *any* $(x, y) \in S$ (i.e., they can interpolate any training sample); however, some (x, y) may be very hard to predict when they are not in the training sample. Such examples may be considered to be “memorised”, as the model could not “generalise” to these examples based on the rest of the training data alone.

Despite its strengths, Equation 1 has an obvious drawback: it is prohibitive to compute in most practical settings. Indeed, it naïvely requires that we retrain our learner at least N times, with *every* training sample excluded once; accounting for randomness in A requires further repetitions. Feldman and Zhang [30] provided a more tractable estimator, wherein for fixed integer M , one draws K *sub-samples* $\{S^{(k)}\}_{k \in [K]}$ uniformly from $\mathcal{P}_M(S)$, the set of all M -sized subsets of S . For fixed (x, y) , let $K_{\text{in}} \doteq \{k \in [K]: (x, y) \in S^{(k)}\}$, and $K_{\text{out}} \doteq \{k \in [K]: (x, y) \notin S^{(k)}\}$ denote the sub-samples including and excluding (x, y) , respectively. We then compute

$$\widehat{\text{mem}}_{M,K}(x, y; S) = \frac{1}{|K_{\text{in}}|} \sum_{k \in K_{\text{in}}} \mathbb{1}[y = A(x; S^{(k)})] - \frac{1}{|K_{\text{out}}|} \sum_{k \in K_{\text{out}}} \mathbb{1}[y = A(x; S^{(k)})]. \quad (2)$$

This quantity estimates $\text{mem}(x, y; S)$ to precision $\mathcal{O}(1/\sqrt{K})$ [30]. Jiang et al. [45] considered a closely related quantity, namely *consistency score* (or *C-score*), defined as $\text{cscore}(x, y; S) = \mathbb{E}_M [\mathbb{E}_{S' \sim \mathcal{P}_M(S)} [\mathbb{P}(y = A(x; S' - \{(x, y)\}))]]$. When M is drawn from a point-mass, this is the second term in $\widehat{\text{mem}}_{M,K}(x, y; S)$. Note that the first term in $\widehat{\text{mem}}_{M,K}(x, y; S)$ is typically 1 for overparameterised models, since they are capable of interpolation. Jiang et al. [45] also proposed effective *proxies* for the C-score, which rely on the model behaviour across training steps. Suppose we have a model that is iteratively trained for steps $t \in \{1, 2, \dots, T\}$, where at t -th step, the model produces a probability distribution $\hat{p}^{(t)}: \mathcal{X} \rightarrow \Delta(\mathcal{Y})$ over the labels. Jiang et al. [45] argued that the metric capturing the temporal average of the probability assigned to the true label:

$$\text{cprox}(x, y; S) = \mathbb{E}_t \left[\hat{p}_y^{(t)}(x) \right] \quad (3)$$

can correlate strongly with (the point mass version of) $\text{cscore}(x, y; S)$.

Resemblance between memorization and example difficulty. Equation 3 provides an interesting bridge between memorisation and *example difficulty*. For example, TraIn [67] and GRAD [65] also use the evolution of model predictions across training steps to identify samples that are difficult to learn; roughly, these are samples which cause large loss updates when they are trained on. Equation 3 is also related to the notion of *forgetting* [75, 88, 56]: a count of the number of transitions from *learned* to *forgotten* during training an example undergoes. Another related metric is the *learning speed*: the earliest training iteration after which the model predicts the ground truth class for that example in all subsequent iterations. A different notion of difficulty introduced by [62] is the *CG score*, which relies on calculating the gap in generalization error bounds of an overparameterized two-layer network with ReLU activations when an example is *excluded* from training. Another related measure of sample difficulty is the RHO-loss [59], wherein the training loss is contrast with the *irreducible* loss when a sample is only present in a holdout set. The C-score also correlates with the *prediction depth* [5], which computes model predictions at intermediate layers, and reports the earliest layer beyond which all predictions are consistent.

In a related line of work, Ghorbani and Zou [31] proposed the *data Shapley score* to capture the value of a training example with respect to a train dataset, a learning algorithm and an evaluation metric. The score differs from the memorisation score in that the impact of an example is evaluated with respect to *all* subsets of the training set, as opposed to the entire training set. Interestingly, this is similar to Equation 2, which samples fixed-size subsets of the training set.

Memorisation versus generalisation. Given that the ultimate goal of statistical learning is *generalisation*, it is natural to ask whether this is at odds with “memorisation”. A classical result establishes that a lookup table as implemented by the k -NN algorithm is universally consistent [74]. Interpolating models such as boosting with decision stumps have similarly been shown to generalise [6], and more refined analyses have been conducted for modern interpolating neural models [7, 28, 16, 9, 61, 50, 60, 8, 76]. Intriguingly, some recent works have established that under certain settings, “memorisation” may be *necessary* for generalisation, either in the sense of interpolation [23], stability-based label memorisation [29], or stronger example-level memorisation [14].

Implicit versus explicit memorisation. Memorisation has received particular interest in the context of large language models (LLMs), such as GPT [15] and T5 [69]. Here, “memorisation” typically refers to the ability of a model to recall factual information present in the training set (e.g., names of individuals) [66, 70, 19, 20]. This aligns with the notion from statistical learning of “memorisation” as employing a lookup table. While LLMs are capable of *implicit* memorisation, several works have shown benefits from augmenting neural models with an *explicit* memorisation component [48, 34, 47, 12, 81]. Similar ideas have also proven useful outside of NLP [63, 76, 78].

Definition	References
Zero training error	[83]
Zero training error + label is random	[3, 82, 73]
Training error below Bayes error rate	[17, 23]
Prediction based on spurious correlations	[71, 32]
Ability to reconstruct from other training samples	[68, 19]
Inability to predict when removed from training sample	[29, 45]

Table 1: Summary of existing definitions of “memorisation” of a training sample. In this paper, we focus on the final row, which proposes a stability-based metric quantifying sample predictability.

Prior empirical analyses of memorisation. Several works have studied the *interpolation* behaviour of neural models as one varies model complexity [83, 61]. Empirical studies of memorisation in the sense of fitting to random (noisy) labels was conducted in [3, 33]. These works demonstrated that real-world networks tend to fit “easy” samples first, and exhibit qualitatively different learning trajectories when presented with clean versus noisy samples. Zhang et al. [84] provided an elegant study of the interplay between memorisation and generalisation for a regression problem, involving learning either a constant or identity function. Feldman and Zhang [30] studied memorisation in the sense of the stability-based memorisation score in Feldman [29] (cf. Equation 1), by quantifying

the influence of each training example on different test examples. Based on these, they identified a subset of test examples for which the model significantly relies on the memorized (in the stability sense) training examples to make correct predictions. While the direct inspiration for our study, these experiments were for a single architecture on CIFAR-100 and ImageNet. Furthermore, they did not consider the impact of model distillation.

Concurrent work [26] analyses the effect of model compression specifically for CIFAR-10 and concur with our findings that compression inhibits memorization. However, like [29], most other works study the memorization behavior individually for each model rather than consolidate trends across a family of models. Han et al. [35] examine what images are typically memorized by a large variety of image classifiers. A line of work [5, 57, 73] has investigated how to localize where an example is memorized in a given network. Other works have looked at the effect of orthogonal factors such as initialization [58] on memorization. Xu et al. [80] examine the interplay between memorization and robustness specifically for adversarially-trained models, while we study standard-trained models.

An orthogonal line of work has extended the concept of memorization to language modeling. Zheng and Jiang [86], Zhang et al. [85] extend the formulation of memorization in Feldman [29] and confirm that the long tail theory holds in language datasets as well. However, most work in language models [21, 4, 11] take a qualitatively different approach to memorisation, wherein a model is said to memorise a datapoint if it can complete a prefix in the same way it was completed in the training set.

3 The unexpected tale of memorisation

To demystify the excellent performance of modern neural networks, a key step is developing a systematic understanding of their fundamental properties as we scale their capacity. It is known that as the model size grows, both the *interpolation* and *generalisation* of the model increase. Given that memorisation is a fundamental related property, it is natural to ask how the memorisation behavior of modern networks evolves with increasing model sizes. In this section, we present a detailed empirical study in this direction, while highlighting various nuanced and surprising observations. Before discussing our key findings, we begin by introducing the exact setup and scope of our empirical study.

3.1 Setup and scope

Quantifying the nature of memorisation requires picking a suitable definition of the term. Owing to its conceptual simplicity and intuitive alignment with the term “memorisation”, we employ the stability based memorisation score of Feldman [29], per Equation 1. For computational tractability, we employ the approximation to this score from Feldman and Zhang [30], per Equation 2. This reduces the computational burden of estimating $\text{mem}(x, y; S)$, but does not eliminate it: for *each* setting of interest, we need to draw a number of independent data sub-samples, and train a fresh model on each. This necessitates a tradeoff between the breadth of results across settings, and the precision of the memorisation scores estimated for any individual result. We favour the former, and estimate $\widehat{\text{mem}}_{M,K}(x, y; S)$ via $K = 400$ draws of sub-samples $S' \sim \mathcal{P}_M(S)$, with $M = \lceil 0.7N \rceil$.

With this setup, we empirically examine a simple question: *how is memorisation influenced by model capacity?* Specifically, for a range of standard image classification datasets — CIFAR-10, CIFAR-100, and Tiny-ImageNet — we empirically quantify the memorisation score as we vary the capacity of standard neural models, based on the ResNet [39, 40] and MobileNet-v3 [44] family (cf. Appendix D for precise settings). Here, it is worth highlighting that while Feldman [29] studied memorisation profiles for fixed models, the *change* in memorisation behavior across model sizes has not been systematically studied before.

In the rest of the section, we present key findings from our empirical study, progressively exploring memorization behavior at a more granular level. We start with discussing the average memorization scores for networks and then present the distribution of memorisation scores across training examples for different sized models. We next explore per-example memorization trajectory across model sizes which leads an intuitive categorization of all training examples into four categories. We conclude with inspecting whether the properties of memorisation we uncover hold under example difficulty metrics which were shown in previous works to highly correlate with the stability based memorisation.

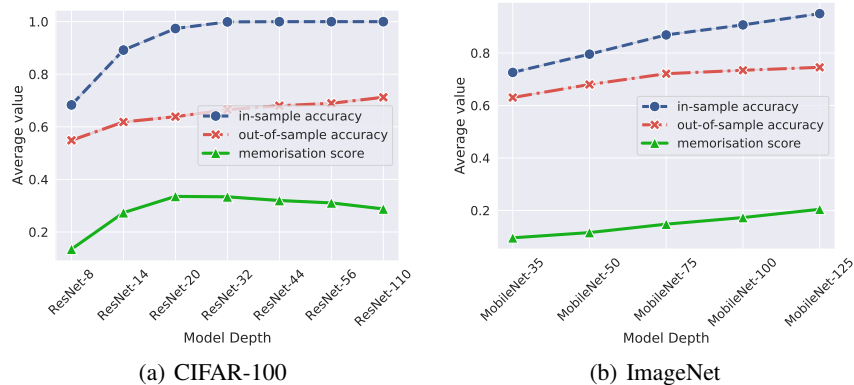


Figure 2: Average memorisation scores from models of varying size trained on CIFAR-100 (left plot) and ImageNet (right plot) training samples. On CIFAR-100, the average memorisation score steadily *increases* with depth up till the ResNet-20, and steadily *decreases* afterwards. The increase up to a certain depth can be explained by the in-sample accuracy increasing faster than out-of-sample accuracy (right plot), until the point where the former is $\sim 100\%$. On ImageNet, the in-sample accuracy does not reach $\sim 100\%$ and in effect the memorisation scores is seen as increasing.

3.2 Sufficiently large models memorise less on average

Previous works have claimed that larger networks imply more memorisation, albeit based on different notion of memorisation than ours [83, 61, 21]. This leads one to hypothesise that average memorisation score across training set, per Equation 1 or 2, should increase with model size. We now assess whether this hypothesis is borne out empirically.

In Figure 2, we visualise how ResNet model depth influences the memorisation score (Equation 2) on CIFAR-100 and ImageNet. Specifically, for each model, we report the *average* memorisation score across all training samples as a coarse summary. For CIFAR-100 we see that this score increases up to depth 20, and then, contrary to the naïve hypothesis above, starts *decreasing* (albeit slightly).

This (initially) puzzling phenomenon may be intuitively understood by breaking down the two terms used to compute the memorisation score in equation 2: the *in-sample accuracy*, and the *out-of-sample accuracy*. As expected, both quantities steadily increase with model depth. The increasing memorisation score up to depth 20 can be explained by the *in-sample accuracy* increasing *faster* than the *out-of-sample accuracy* up to this point; beyond this point, the in-sample accuracy saturates at 100%, while the out-of-sample accuracy keeps increasing. Thus, necessarily, the memorisation score starts to drop. In Appendix H.3, we give an alternative explanation for why memorisation decreases after interpolation. For ImageNet, we see memorisation steadily increasing due to in-sample accuracy increasing faster than out-of-sample accuracy, while the in-sample accuracy does not saturate.

3.3 Large models have increasingly bi-modal memorisation score distributions

The result of memorisation decreasing with an increasing model size discussed in Section 3.2 only considered the *average* memorisation score for a given model. But how does the *distribution* of memorisation scores vary with model capacity? To this end, Figure 3 plots precisely this distribution for each model in consideration. We observe that the memorisation scores tend to be *bi-modal*, with most samples' score being closer to 0 or 1. This is in agreement with observations made by Feldman and Zhang [30] for a *fixed* architecture: ResNet on CIFAR-100 and MobileNet on ImageNet.

More interestingly, our finding is that this bi-modality is *exaggerated with model depth*: larger models have a higher fraction of samples with both memorisation score close to 0 and 1. The increase of samples with high memorisation score denotes an increasing generalisation gap on a subset of training points. We find this to be true across various datasets and architectures, as shown in Figure 6 (Appendix). While the increasing fraction of samples with low memorisation score is consistent with the finding on CIFAR-100 about the average memorisation score decreasing, it is surprising that there is also a subset of points with *increasing* memorisation.

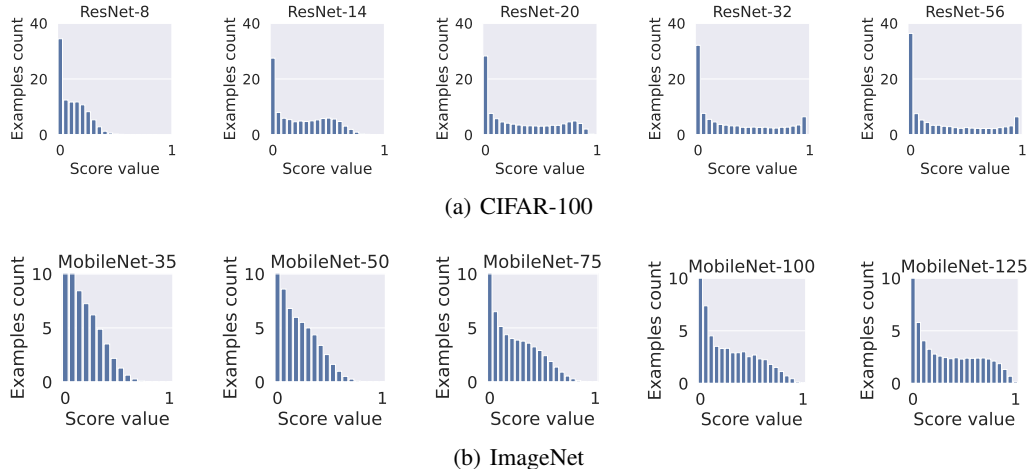


Figure 3: Distributions of memorisation scores from models trained on CIFAR-100 (top row) and ImageNet (bottom row) training samples. As model size increases, relatively more samples are highly memorised (notice the hump in the graphs from the top row is being progressively pushed to the right); Further, the number of examples with very low memorisation increases as well. Overall, we find a growing *bi-modality* of the distribution of memorisation scores with increasing size. In Figure 6 (Appendix), we show that the bi-modality of the memorisation score holds across more datasets (CIFAR-10, CIFAR-100, ImageNet, TinyImageNet) and model families (ResNet, MobileNet) and in Figure 7 we show this when varying model widths (as opposed to depths) to increase model sizes.

3.4 On the diversity of memorisation trajectories over model sizes

The bi-modality of the memorisation scores that we observed in Section 3.3 suggests that there exist at least two kinds of examples: those whose memorisation scores increase with depth, and those whose scores decrease. Next, we seek to more carefully characterize what these examples are by analysing the trajectory of memorisation score for *individual* examples.

Categorizing examples by their memorisation trajectories. In Figure 1, we report the average memorisation score as a function of model depth (size) for individual examples from the *sunflower* class of CIFAR-100 (see Appendix for presentation over more classes and across different classes, upholding our observations, as well as from the ImageNet models). We find four different kinds of trajectory patterns: increasing, decreasing, cap-shaped and constant. Also, in Table 12 (Appendix) we report predictions for the shown examples.

α	constant	increasing	decreasing	cap-shaped	other
0.05	0.243	0.175	0.145	0.316	0.121
0.10	0.395	0.298	0.105	0.187	0.016

Table 2: Counts of examples in the CIFAR-100 data as broken down by the trajectory type. For robust counting, we treat a change in memorization by less than α as a no change.

In Table 2 we report counts of examples in the CIFAR-100 data broken down by the trajectory they exhibit across model sizes. For robust counting, we treat a change in memorization by less than 0.1 as a no change. We can see how the four trajectory types we present cover the majority of example trajectories.

Interpreting the example trajectories. We next offer a qualitative characterisation of the samples from the four trajectory types we identified. Such qualitative grouping of samples is common in work studying *example difficulty* [5, 45, 30]. We first notice that the least-changing memorisation examples are *easy and unambiguous*. Quantitatively as well, we find that amongst these examples, the peak memorisation score tends to be low (i.e., such samples tend to consistently not be memorised), suggesting that these are easy and unambiguous points. This phenomenon is also evident in Figure 9 (Appendix), where the examples with the least changing memorisation score are also least memorised scores by individual models. Next, we note that the examples corresponding to *increasing, cap-shaped* and *decreasing* memorisation trajectories are hard and ambiguous (cf. Figure 1). The *decreasing* and

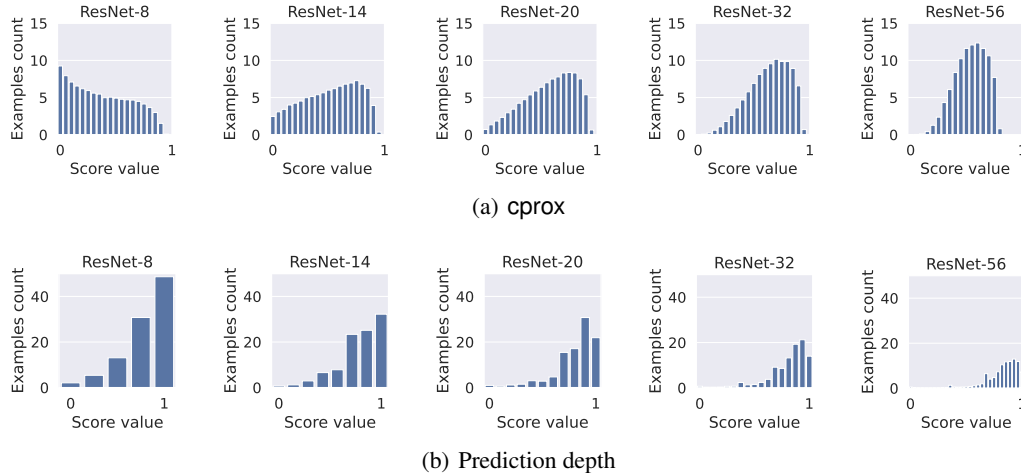


Figure 4: Distributions of C-proxy scores (top row; see Equation (3)) and prediction depth (bottom row; see [5] and Appendix J for the details of our implementation) from models trained on CIFAR-100 training samples. Although these have high correlation with memorisation scores, as promised in prior work, they fail to capture the bi-modal behavior of memorisation.

cap-shaped examples are arguably hard but with the ground-truth label correctly assigned in the data. On the other hand, the *increasing* examples are often multi-labeled (e.g., the first *increasing* example containing a bee) or mislabeled (e.g. the third *increasing* example), such that a human rater could be unlikely to label these images with the dataset provided label. This parallels the predictions from ResNet-110 for these examples, which are arguably no less reasonable than the label as presented in the dataset, as can be observed in Table 12 (Appendix). We inspect more examples and further elaborate on our observations in Appendix H.

3.5 Do memorisation score proxies exhibit the same trends?

As discussed in Section 2, the stability-based memorisation score is difficult to compute. The C-score proxy *cprox* (Equation 3) was proposed in Jiang et al. [45] as a computationally efficient alternative to the C-score, a metric closely related to the stability-based memorisation score of Equation 1. Indeed, Jiang et al. [45] found this measure to have high *correlation* with the C-score, while cautioning that it should not be interpreted as an *approximation* to more fine-grained characteristics of the latter.

Going beyond correlation, however, we find in Figure 4 that the distribution of *cprox* scores have markedly different characteristics to stability-based memorisation: the former are *unimodal*, with most samples having a high score value. Recall that by contrast, stability-based memorisation scores exhibit a bi-modal distribution, with this phenomenon exaggerated with increasing model size (see Figure 3). Consequently, we do not observe many of the unexpected trends exhibited by stability-based memorisation, e.g., the possibility of *cprox* systematically *decreasing* for some samples as depth increases. We also report distributions from the example difficult metric called *prediction depth*, which has been shown to be closely related to the C-score, and analogously find that prediction depth yields a very different distribution than memorisation score (see Appendix).

Overall, we view the above discrepancy as an instance of the famous *Anscombe’s quartet* [2] in statistics: it is possible for two distributions to have very similar correlation statistics, but for the distributions themselves to be visually dissimilar. Thus, we conclude it is important to be cautious about conclusions drawn from a high correlation between various memorization scores and their proxies, as they may in reality be capturing different properties of data.

4 Distillation lowers memorisation

Despite the impressive performance of large neural models on a range of challenging tasks in vision and NLP, practical deployment of such models is often infeasible due to their high inference cost.

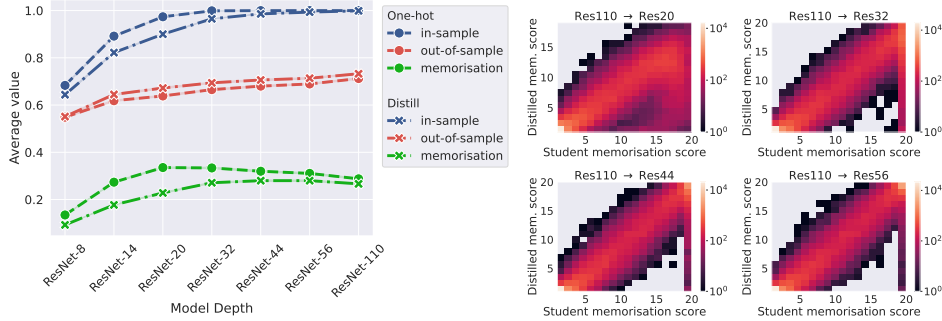


Figure 5: Left: Average memorisation score is reduced by distillation across model depths, which can be attributed to both the reduced in-sample accuracy and increased out-of-sample accuracy. Figure shows average memorisation scores from one-hot and distilled models on CIFAR-100 training samples. Right: Distillation inhibits memorisation of the student: each plot shows the joint density of memorisation scores under a standard model, and one distilled from a ResNet-110 teacher. As the gap between teacher and student models becomes wider, samples memorised by the student see a sharp decrease in memorisation score under distillation (see the vertical bar at right end of plot). Notably, distillation does not affect other samples as strongly.

Recently, *knowledge distillation* [18, 41] has emerged as a promising approach to compress these large models into more tractable models. Here, one feeds a large (“teacher”) model’s predicted *distribution* over labels as the prediction targets for a small (“student”) model. Compared to the standard training on raw labels (as considered in earlier sections), distillation can provide significant performance gains; these are informally attributed to distillation performing “knowledge transfer”. Knowledge distillation has been successfully applied across many applications, including: computer vision [10], language modeling [72], information retrieval [51], machine translation [87], and ads recommendation [1, 52].

Compared to standard training, distillation presents us with an interesting setup where models of different sizes interact during the training procedure. This prompts us to ask: how does coupling between models of different sizes during distillation affect, if at all, the memorisation behavior of the resulting student model? Interestingly, while distillation has been shown to yield significant performance gains on average, *training accuracy* has been shown to be systematically harmed [24]. Previous work also showed how distillation can lead to worsened *accuracy* on a subset of hard examples [54]. In a related study, model compression has been shown to harm *accuracy* on tail classes [42]. These observations indeed hint at the potential impact of distillation procedure on student’s memorisation behavior, which we systematically explore in this section.

Towards this, we consider knowledge distillation as conducted using logit matching, and where the teacher is trained on the same sub-sample as the student for estimating the memorisation scores per Equation 2. We provide the hyperparameter details in Appendix D.

Distillation inhibits memorisation on average. We begin by investigating what happens to average memorisation under distillation. As discussed earlier, distillation is known to reduce the train accuracy compared to the one-hot models, while increasing the test accuracy [24]; in Table 6 (Appendix), we report the train and test accuracies. From this, one could expect distillation to inhibit memorisation. In Figure 5 (left), we illustrate the difference in distributions of memorisation scores across models trained on the ground truth labels (which we call *one-hot training*) and the models distilled from a ResNet-110 teacher model. As expected, we find that distillation tends to *reduce* the number of memorised samples. From the decomposition of memorisation into in-sample and out-sample accuracies for the one-hot and distilled models, we find that the in-sample accuracy becomes lower and out-of-sample accuracy becomes higher under distillation. This parallels the observation that train accuracy lowers, and test accuracy increases under distillation.

Distillation inhibits memorisation of highly memorised examples. We next turn to analysing the distribution of per-example change in memorisation under distillation. In Figure 5 (right), we report the joint density of memorisation scores under a standard model, and one distilled from a ResNet-110

teacher. We can see that distillation inhibits memorisation particularly for the examples highly memorised by the one-hot model, and especially when the teacher-student gap is wide. Interestingly, none of the examples with small memorisation score from the one-hot model obtain a significant *increase* in memorisation from distillation.

In the Appendix, we also show on per-example trajectories how memorisation lowers especially for the challenging and ambiguous examples, which often get high memorisation score value by either the small or large models (Figure 14 and Figure 15; Appendix). In the Appendix, we report further results showing how memorisation is overall lowered across different student and teacher models (Figure 18; Appendix).

Why distillation reduces memorisation but improves generalisation?

Our finding is that distillation reduces memorisation but improves generalisation, which is intriguing since recent works suggest memorisation can be beneficial for generalisation [29]. To address this apparent conflict, below we report an analysis of what examples distillation reduces memorisation on. Our hypothesis is that distillation reduces memorisation mostly on hardest examples, and thus releases the generalisation capacity for the model to perform better on other, easier to learn examples.

To verify this hypothesis, in Table 3 we provide the breakdown of the CIFAR-100 train data into different categories’ counts over the dataset (as defined in Figure 1). In particular, we fix the teacher-student pair of ResNet-110 and ResNet-32 and consider the set of examples S where the memorisation score reduces compared to the one-hot student (one-hot ResNet-32 in the above example). We find that memorization is mostly reduced by distillation on the examples with an increasing memorisation trajectory examples, which consist of ambiguous and noisy examples (as we note in Section 3.4). Note that this observation relates to the empirical observations about distillation being beneficial in noisy label scenarios [53].

Examples set	constant	increasing	decreasing	cap-shaped	other
All examples	0.243	0.175	0.145	0.316	0.121
Reduced memorisation	0.000	0.972	0.000	0.023	0.005

Table 3: Counts of examples in the CIFAR-100 data as broken down by the trajectory type. The examples where distillation reduces memorisation (as measured by comparing memorisation between the distilled and one-hot trained ResNet-32 models, while using ResNet-110 as the teacher model) are mostly increasing in their trajectory.

5 Discussion and practical implication

Our study leads to important practical conclusions and avenues for future works. First, one should be careful with using certain statistics as proxies for memorisation. Previous works suggested that various quantities defined based on model training or model inference can provide efficient proxies for memorisation score. Although these proxies appear to yield high correlation to memorisation, we find that distributionally they are significantly different, and do not capture the key aspects of the memorisation behavior of practical models that we uncover. This points at a future direction of identifying reliable memorisation score proxies which can be efficiently computed.

Previous works have categorized the difficulty of examples [29, 5, 45] upon fixing a specific model size. Our analysis points at the importance of characterising examples by taking into account multiple model sizes. For instance, Feldman [29] refer to examples that have high memorization score for a particular architecture as the long tail examples for a given dataset. As our analysis reveals, what is memorised for one model size, may not be for a different size.

References

[1] Rohan Anil, Sandra Gado, Da Huang, Nijith Jacob, Zhuoshu Li, Dong Lin, Todd Phillips, Cristina Pop, Kevin Regan, Gil I. Shamir, Rakesh Shivanna, and Qiqi Yan. On the factory floor: ML engineering for industrial-scale ads recommendation models, 2022. URL <https://arxiv.org/abs/2209.05310>.

[2] F. J. Anscombe. Graphs in statistical analysis. *The American Statistician*, 27(1):17–21, 1973. doi: 10.1080/00031305.1973.10478966. URL <https://www.tandfonline.com/doi/abs/10.1080/00031305.1973.10478966>.

- [3] Devansh Arpit, Stanisław Jastrzebski, Nicolas Ballas, David Krueger, Emmanuel Bengio, Maxinder S. Kanwal, Tegan Maharaj, Asja Fischer, Aaron Courville, Yoshua Bengio, and Simon Lacoste-Julien. A closer look at memorization in deep networks. In *Proceedings of the 34th International Conference on Machine Learning - Volume 70, ICML'17*, pages 233–242. JMLR.org, 2017.
- [4] Ching-Yuan Bai, Hsuan-Tien Lin, Colin Raffel, and Wendy Chi-wen Kan. On training sample memorization: Lessons from benchmarking generative modeling with a large-scale competition. In Feida Zhu, Beng Chin Ooi, and Chunyan Miao, editors, *KDD '21: The 27th ACM SIGKDD Conference on Knowledge Discovery and Data Mining, 2021*, pages 2534–2542. ACM, 2021.
- [5] Robert John Nicholas Baldock, Hartmut Maennel, and Behnam Neyshabur. Deep learning through the lens of example difficulty. In *NeurIPS*, 2021. URL <https://arxiv.org/abs/2106.09647>.
- [6] Peter Bartlett, Yoav Freund, Wee Sun Lee, and Robert E. Schapire. Boosting the margin: a new explanation for the effectiveness of voting methods. *The Annals of Statistics*, 26(5):1651–1686, 1998. doi: 10.1214/aos/1024691352. URL <https://doi.org/10.1214/aos/1024691352>.
- [7] Peter L. Bartlett, Dylan J. Foster, and Matus Telgarsky. Spectrally-normalized margin bounds for neural networks. In Isabelle Guyon, Ulrike von Luxburg, Samy Bengio, Hanna M. Wallach, Rob Fergus, S. V. N. Vishwanathan, and Roman Garnett, editors, *Advances in Neural Information Processing Systems 30: Annual Conference on Neural Information Processing Systems 2017, December 4-9, 2017, Long Beach, CA, USA*, pages 6240–6249, 2017.
- [8] Peter L. Bartlett, Philip M. Long, Gábor Lugosi, and Alexander Tsigler. Benign overfitting in linear regression. *Proceedings of the National Academy of Sciences*, 117(48):30063–30070, 2020. doi: 10.1073/pnas.1907378117. URL <https://www.pnas.org/doi/abs/10.1073/pnas.1907378117>.
- [9] Mikhail Belkin, Daniel Hsu, and Partha P. Mitra. Overfitting or perfect fitting? risk bounds for classification and regression rules that interpolate. In *Proceedings of the 32nd International Conference on Neural Information Processing Systems, NIPS'18*, pages 2306–2317, Red Hook, NY, USA, 2018. Curran Associates Inc.
- [10] Lucas Beyer, Xiaohua Zhai, Amélie Royer, Larisa Markeeva, Rohan Anil, and Alexander Kolesnikov. Knowledge distillation: A good teacher is patient and consistent, 2021.
- [11] Stella Biderman, USVSN Sai Prashanth, Lintang Sutawika, Hailey Schoelkopf, Quentin Anthony, Shivanshu Purohit, and Edward Raff. Emergent and predictable memorization in large language models. *CoRR*, abs/2304.11158, 2023. URL <https://doi.org/10.48550/arXiv.2304.11158>.
- [12] Sebastian Borgeaud, Arthur Mensch, Jordan Hoffmann, Trevor Cai, Eliza Rutherford, Katie Millican, George van den Driessche, Jean-Baptiste Lespiau, Bogdan Damoc, Aidan Clark, Diego de Las Casas, Aurelia Guy, Jacob Menick, Roman Ring, Tom Hennigan, Saffron Huang, Loren Maggiore, Chris Jones, Albin Cassirer, Andy Brock, Michela Paganini, Geoffrey Irving, Oriol Vinyals, Simon Osindero, Karen Simonyan, Jack W. Rae, Erich Elsen, and Laurent Sifre. Improving language models by retrieving from trillions of tokens. *CoRR*, abs/2112.04426, 2021. URL <https://arxiv.org/abs/2112.04426>.
- [13] Olivier Bousquet and André Elisseeff. Stability and generalization. *Journal of Machine Learning Research*, 2:499–526, 2002.
- [14] Gavin Brown, Mark Bun, Vitaly Feldman, Adam Smith, and Kunal Talwar. When is memorization of irrelevant training data necessary for high-accuracy learning? In *Proceedings of the 53rd Annual ACM SIGACT Symposium on Theory of Computing, STOC 2021*, page 123–132, New York, NY, USA, 2021. Association for Computing Machinery. ISBN 9781450380539. doi: 10.1145/3406325.3451131. URL <https://doi.org/10.1145/3406325.3451131>.

- [15] Tom B. Brown, Benjamin Mann, Nick Ryder, Melanie Subbiah, Jared Kaplan, Prafulla Dhariwal, Arvind Neelakantan, Pranav Shyam, Girish Sastry, Amanda Askell, Sandhini Agarwal, Ariel Herbert-Voss, Gretchen Krueger, Tom Henighan, Rewon Child, Aditya Ramesh, Daniel M. Ziegler, Jeffrey Wu, Clemens Winter, Christopher Hesse, Mark Chen, Eric Sigler, Mateusz Litwin, Scott Gray, Benjamin Chess, Jack Clark, Christopher Berner, Sam McCandlish, Alec Radford, Ilya Sutskever, and Dario Amodei. Language models are few-shot learners. *CoRR*, abs/2005.14165, 2020. URL <https://arxiv.org/abs/2005.14165>.
- [16] Alon Brutzkus, Amir Globerson, Eran Malach, and Shai Shalev-Shwartz. SGD learns over-parameterized networks that provably generalize on linearly separable data. In *International Conference on Learning Representations*, 2018. URL <https://openreview.net/forum?id=rJ33wwxRb>.
- [17] Sébastien Bubeck, Ronen Eldan, Yin Tat Lee, and Dan Mikulincer. Network size and weights size for memorization with two-layers neural networks. In *Proceedings of the 34th International Conference on Neural Information Processing Systems*, NIPS’20, Red Hook, NY, USA, 2020. Curran Associates Inc. ISBN 9781713829546.
- [18] Cristian Bucilă, Rich Caruana, and Alexandru Niculescu-Mizil. Model compression. In *Proceedings of the 12th ACM SIGKDD International Conference on Knowledge Discovery and Data Mining*, KDD ’06, pages 535–541, New York, NY, USA, 2006. ACM.
- [19] Nicholas Carlini, Florian Tramèr, Eric Wallace, Matthew Jagielski, Ariel Herbert-Voss, Katherine Lee, Adam Roberts, Tom Brown, Dawn Song, Úlfar Erlingsson, Alina Oprea, and Colin Raffel. Extracting training data from large language models. In *30th USENIX Security Symposium (USENIX Security 21)*, pages 2633–2650. USENIX Association, August 2021. ISBN 978-1-939133-24-3. URL <https://www.usenix.org/conference/usenixsecurity21/presentation/carlini-extracting>.
- [20] Nicholas Carlini, Daphne Ippolito, Matthew Jagielski, Katherine Lee, Florian Tramer, and Chiyuan Zhang. Quantifying memorization across neural language models, 2022. URL <https://arxiv.org/abs/2202.07646>.
- [21] Nicholas Carlini, Daphne Ippolito, Matthew Jagielski, Katherine Lee, Florian Tramer, and Chiyuan Zhang. Quantifying memorization across neural language models. In *The Eleventh International Conference on Learning Representations*, 2023. URL https://openreview.net/forum?id=TatRHT_1cK.
- [22] Satrajit Chatterjee. Learning and memorization. In Jennifer Dy and Andreas Krause, editors, *Proceedings of the 35th International Conference on Machine Learning*, volume 80 of *Proceedings of Machine Learning Research*, pages 755–763. PMLR, 10–15 Jul 2018. URL <https://proceedings.mlr.press/v80/chatterjee18a.html>.
- [23] Chen Cheng, John Duchi, and Rohith Kudipudi. Memorize to generalize: on the necessity of interpolation in high dimensional linear regression, 2022. URL <https://arxiv.org/abs/2202.09889>.
- [24] J. H. Cho and B. Hariharan. On the efficacy of knowledge distillation. In *2019 IEEE/CVF International Conference on Computer Vision (ICCV)*, pages 4793–4801, 2019.
- [25] Jeremy M Cohen, Elan Rosenfeld, and J. Zico Kolter. Certified adversarial robustness via randomized smoothing, 2019. URL <https://arxiv.org/abs/1902.02918>.
- [26] Harvey Dam, Vinu Joseph, Aditya Bhaskara, Ganesh Gopalakrishnan, Saurav Muralidharan, and Michael Garland. Understanding the effect of the long tail on neural network compression. *CoRR*, abs/2306.06238, 2023. URL <https://doi.org/10.48550/arXiv.2306.06238>.
- [27] L. Devroye, L. Györfi, and G. Lugosi. *A probabilistic theory of pattern recognition*. Springer, 1996.

- [28] Gintare Karolina Dziugaite and Daniel M. Roy. Computing nonvacuous generalization bounds for deep (stochastic) neural networks with many more parameters than training data. In *Proceedings of the 33rd Annual Conference on Uncertainty in Artificial Intelligence (UAI)*, 2017.
- [29] Vitaly Feldman. Does learning require memorization? A short tale about a long tail. *CoRR*, abs/1906.05271, 2019. URL <http://arxiv.org/abs/1906.05271>.
- [30] Vitaly Feldman and Chiyuan Zhang. What neural networks memorize and why: Discovering the long tail via influence estimation. In H. Larochelle, M. Ranzato, R. Hadsell, M.F. Balcan, and H. Lin, editors, *Advances in Neural Information Processing Systems*, volume 33, pages 2881–2891. Curran Associates, Inc., 2020. URL <https://proceedings.neurips.cc/paper/2020/file/1e14bfe2714193e7af5abc64ecbd6b46-Paper.pdf>.
- [31] Amirata Ghorbani and James Zou. Data shapley: Equitable valuation of data for machine learning. In Kamalika Chaudhuri and Ruslan Salakhutdinov, editors, *Proceedings of the 36th International Conference on Machine Learning*, volume 97 of *Proceedings of Machine Learning Research*, pages 2242–2251. PMLR, 09–15 Jun 2019. URL <https://proceedings.mlr.press/v97/ghorbani19c.html>.
- [32] Margalit Glasgow, Colin Wei, Mary Wootters, and Tengyu Ma. Max-margin works while large margin fails: Generalization without uniform convergence, 2022. URL <https://arxiv.org/abs/2206.07892>.
- [33] Jindong Gu and Volker Tresp. Neural network memorization dissection. *CoRR*, abs/1911.09537, 2019. URL <http://arxiv.org/abs/1911.09537>.
- [34] Kelvin Guu, Kenton Lee, Zora Tung, Panupong Pasupat, and Ming-Wei Chang. Realm: Retrieval-augmented language model pre-training. In *Proceedings of the 37th International Conference on Machine Learning, ICML’20*. JMLR.org, 2020.
- [35] Junlin Han, Huangying Zhan, Jie Hong, Pengfei Fang, Hongdong Li, Lars Petersson, and Ian D. Reid. What images are more memorable to machines? *CoRR*, 2022. doi: 10.48550/arXiv.2211.07625. URL <https://doi.org/10.48550/arXiv.2211.07625>.
- [36] Trevor Hastie, Robert Tibshirani, and Jerome Friedman. *The Elements of Statistical Learning*. Springer Series in Statistics. Springer New York Inc., New York, NY, USA, 2001.
- [37] K. He, X. Zhang, S. Ren, and J. Sun. Deep residual learning for image recognition. In *2016 IEEE Conference on Computer Vision and Pattern Recognition (CVPR)*, 2016.
- [38] Kaiming He, Xiangyu Zhang, Shaoqing Ren, and Jian Sun. Deep residual learning for image recognition. In *2016 IEEE Conference on Computer Vision and Pattern Recognition (CVPR)*, pages 770–778, 2016. doi: 10.1109/CVPR.2016.90.
- [39] Kaiming He, Xiangyu Zhang, Shaoqing Ren, and Jian Sun. Deep residual learning for image recognition. In *Proceedings of the IEEE Conference on Computer Vision and Pattern Recognition (CVPR)*, June 2016.
- [40] Kaiming He, Xiangyu Zhang, Shaoqing Ren, and Jian Sun. Identity mappings in deep residual networks. In Bastian Leibe, Jiri Matas, Nicu Sebe, and Max Welling, editors, *Computer Vision – ECCV 2016*, pages 630–645, Cham, 2016. Springer International Publishing. ISBN 978-3-319-46493-0.
- [41] Geoffrey E. Hinton, Oriol Vinyals, and Jeffrey Dean. Distilling the knowledge in a neural network. *CoRR*, abs/1503.02531, 2015.
- [42] Sara Hooker, Aaron Courville, Gregory Clark, Yann Dauphin, and Andrea Frome. What do compressed deep neural networks forget?, 2019. URL <https://arxiv.org/abs/1911.05248>.

- [43] Andrew Howard, Ruoming Pang, Hartwig Adam, Quoc V. Le, Mark Sandler, Bo Chen, Weijun Wang, Liang-Chieh Chen, Mingxing Tan, Grace Chu, Vijay Vasudevan, and Yukun Zhu. Searching for mobilenetv3. In *2019 IEEE/CVF International Conference on Computer Vision, ICCV 2019, Seoul, Korea (South), October 27 - November 2, 2019*, pages 1314–1324. IEEE, 2019. doi: 10.1109/ICCV.2019.00140. URL <https://doi.org/10.1109/ICCV.2019.00140>.
- [44] Andrew Howard, Mark Sandler, Grace Chu, Liang-Chieh Chen, Bo Chen, Mingxing Tan, Weijun Wang, Yukun Zhu, Ruoming Pang, Vijay Vasudevan, Quoc V. Le, and Hartwig Adam. Searching for MobileNetV3. In *Proceedings of the IEEE/CVF International Conference on Computer Vision (ICCV)*, October 2019.
- [45] Ziheng Jiang, Chiyuan Zhang, Kunal Talwar, and Michael C. Mozer. Characterizing structural regularities of labeled data in overparameterized models. In Marina Meila and Tong Zhang, editors, *Proceedings of the 38th International Conference on Machine Learning, ICML 2021, 18-24 July 2021, Virtual Event*, volume 139 of *Proceedings of Machine Learning Research*, pages 5034–5044. PMLR, 2021. URL <http://proceedings.mlr.press/v139/jiang21k.html>.
- [46] Ziheng Jiang, Chiyuan Zhang, Kunal Talwar, and Michael C. Mozer. Characterizing structural regularities of labeled data in overparameterized models, 2021.
- [47] Urvashi Khandelwal, Omer Levy, Dan Jurafsky, Luke Zettlemoyer, and Mike Lewis. Generalization through memorization: Nearest neighbor language models. In *International Conference on Learning Representations*, 2020. URL <https://openreview.net/forum?id=Hk1BjCEKvH>.
- [48] Guillaume Lample, Alexandre Sablayrolles, Marc’Aurelio Ranzato, Ludovic Denoyer, and Hervé Jégou. Large memory layers with product keys. In Hanna M. Wallach, Hugo Larochelle, Alina Beygelzimer, Florence d’Alché-Buc, Emily B. Fox, and Roman Garnett, editors, *Advances in Neural Information Processing Systems 32: Annual Conference on Neural Information Processing Systems 2019, NeurIPS 2019, December 8-14, 2019, Vancouver, BC, Canada*, pages 8546–8557, 2019. URL <https://proceedings.neurips.cc/paper/2019/hash/9d8df73a3cfbf3c5b47bc9b50f214aff-Abstract.html>.
- [49] Yann LeCun, Léon Bottou, Yoshua Bengio, and Patrick Haffner. Gradient-based learning applied to document recognition. *Proceedings of the IEEE*, 86(11):2278–2324, 1998.
- [50] Tengyuan Liang and Alexander Rakhlin. Just interpolate: Kernel “Ridgeless” regression can generalize. *The Annals of Statistics*, 48(3):1329 – 1347, 2020. doi: 10.1214/19-AOS1849. URL <https://doi.org/10.1214/19-AOS1849>.
- [51] Sheng-Chieh Lin, Jheng-Hong Yang, and Jimmy Lin. In-batch negatives for knowledge distillation with tightly-coupled teachers for dense retrieval. In *Proceedings of the 6th Workshop on Representation Learning for NLP (RePLANLP-2021)*, pages 163–173, Online, August 2021. Association for Computational Linguistics. doi: 10.18653/v1/2021.repl4nlp-1.17. URL <https://aclanthology.org/2021.repl4nlp-1.17>.
- [52] Congcong Liu, Yuejiang Li, Jian Zhu, Xiwei Zhao, Changping Peng, Zhangang Lin, and Jingping Shao. Rethinking position bias modeling with knowledge distillation for ctr prediction, 2022. URL <https://arxiv.org/abs/2204.00270>.
- [53] Michal Lukasik, Srinadh Bhojanapalli, Aditya Krishna Menon, and Sanjiv Kumar. Does label smoothing mitigate label noise? In *Proceedings of the 37th International Conference on Machine Learning*, volume 119 of *Proceedings of Machine Learning Research*, pages 6448–6458. PMLR, 2020.
- [54] Michal Lukasik, Srinadh Bhojanapalli, Aditya Krishna Menon, and Sanjiv Kumar. Teacher’s pet: understanding and mitigating biases in distillation. *CoRR*, abs/2106.10494, 2021. URL <https://arxiv.org/abs/2106.10494>.
- [55] Aleksander Madry, Aleksandar Makelov, Ludwig Schmidt, Dimitris Tsipras, and Adrian Vladu. Towards deep learning models resistant to adversarial attacks. In *6th International Conference on Learning Representations, ICLR 2018, Vancouver, BC, Canada, April 30 - May 3, 2018*,

- Conference Track Proceedings*. OpenReview.net, 2018. URL <https://openreview.net/forum?id=rJzIBfZAb>.
- [56] Pratyush Maini, Saurabh Garg, Zachary C. Lipton, and J. Zico Kolter. Characterizing datapoints via second-split forgetting. In *NeurIPS*, 2022. URL http://papers.nips.cc/paper_files/paper/2022/hash/c20447998d6c624b4b97d4466a3bfff5-Abstract-Conference.html.
- [57] Pratyush Maini, Michael Curtis Mozer, Hanie Sedghi, Zachary Chase Lipton, J. Zico Kolter, and Chiyuan Zhang. Can neural network memorization be localized? In *International Conference on Machine Learning, ICML 2023, 23-29 July 2023*, volume 202 of *Proceedings of Machine Learning Research*, pages 23536–23557. PMLR, 2023. URL <https://proceedings.mlr.press/v202/maini23a.html>.
- [58] Harsh Mehta, Ashok Cutkosky, and Behnam Neyshabur. Extreme memorization via scale of initialization. In *9th International Conference on Learning Representations, ICLR 2021*. OpenReview.net, 2021. URL <https://openreview.net/forum?id=Z4R1vxLbRLO>.
- [59] Sören Mindermann, Jan M Brauner, Muhammed T Razzak, Mrinank Sharma, Andreas Kirsch, Winnie Xu, Benedikt Höltingen, Aidan N Gomez, Adrien Morisot, Sebastian Farquhar, and Yarin Gal. Prioritized training on points that are learnable, worth learning, and not yet learnt. In Kamalika Chaudhuri, Stefanie Jegelka, Le Song, Csaba Szepesvari, Gang Niu, and Sivan Sabato, editors, *Proceedings of the 39th International Conference on Machine Learning*, volume 162 of *Proceedings of Machine Learning Research*, pages 15630–15649. PMLR, 17–23 Jul 2022. URL <https://proceedings.mlr.press/v162/mindermann22a.html>.
- [60] Andrea Montanari and Yiqiao Zhong. The interpolation phase transition in neural networks: Memorization and generalization under lazy training, 2020. URL <https://arxiv.org/abs/2007.12826>.
- [61] Behnam Neyshabur, Zhiyuan Li, Srinadh Bhojanapalli, Yann LeCun, and Nathan Srebro. The role of over-parametrization in generalization of neural networks. In *7th International Conference on Learning Representations, ICLR 2019, New Orleans, LA, USA, May 6-9, 2019*. OpenReview.net, 2019.
- [62] Ki Nohyun, Hoyong Choi, and Hye Won Chung. Data valuation without training of a model. In *The Eleventh International Conference on Learning Representations*, 2023. URL <https://openreview.net/forum?id=XIzO8zr-WbM>.
- [63] Rina Panigrahy, Xin Wang, and Manzil Zaheer. Sketch based memory for neural networks. In Arindam Banerjee and Kenji Fukumizu, editors, *Proceedings of The 24th International Conference on Artificial Intelligence and Statistics*, volume 130 of *Proceedings of Machine Learning Research*, pages 3169–3177. PMLR, 13–15 Apr 2021. URL <https://proceedings.mlr.press/v130/panigrahy21a.html>.
- [64] Nicolas Papernot, Patrick D. McDaniel, Xi Wu, Somesh Jha, and Ananthram Swami. Distillation as a defense to adversarial perturbations against deep neural networks. In *IEEE Symposium on Security and Privacy, SP 2016, San Jose, CA, USA, May 22-26, 2016*, pages 582–597, 2016.
- [65] Mansheej Paul, Surya Ganguli, and Gintare Karolina Dziugaite. Deep learning on a data diet: Finding important examples early in training. In M. Ranzato, A. Beygelzimer, Y. Dauphin, P.S. Liang, and J. Wortman Vaughan, editors, *Advances in Neural Information Processing Systems*, volume 34, pages 20596–20607. Curran Associates, Inc., 2021. URL <https://proceedings.neurips.cc/paper/2021/file/ac56f8fe9eea3e4a365f29f0f1957c55-Paper.pdf>.
- [66] Fabio Petroni, Tim Rocktäschel, Sebastian Riedel, Patrick Lewis, Anton Bakhtin, Yuxiang Wu, and Alexander Miller. Language models as knowledge bases? In *Proceedings of the 2019 Conference on Empirical Methods in Natural Language Processing and the 9th International Joint Conference on Natural Language Processing (EMNLP-IJCNLP)*, pages 2463–2473, Hong Kong, China, November 2019. Association for Computational Linguistics. doi: 10.18653/v1/D19-1250. URL <https://aclanthology.org/D19-1250>.

- [67] Garima Pruthi, Frederick Liu, Satyen Kale, and Mukund Sundararajan. Estimating training data influence by tracing gradient descent. In Hugo Larochelle, Marc’Aurelio Ranzato, Raia Hadsell, Maria-Florina Balcan, and Hsuan-Tien Lin, editors, *Advances in Neural Information Processing Systems 33: Annual Conference on Neural Information Processing Systems 2020, NeurIPS 2020, December 6-12, 2020, virtual*, 2020. URL <https://proceedings.neurips.cc/paper/2020/hash/e6385d39ec9394f2f3a354d9d2b88eec-Abstract.html>.
- [68] Adityanarayanan Radhakrishnan, Mikhail Belkin, and Caroline Uhler. Overparameterized neural networks implement associative memory. *Proceedings of the National Academy of Sciences*, 117(44):27162–27170, 2020. doi: 10.1073/pnas.2005013117. URL <https://www.pnas.org/doi/abs/10.1073/pnas.2005013117>.
- [69] Colin Raffel, Noam Shazeer, Adam Roberts, Katherine Lee, Sharan Narang, Michael Matena, Yanqi Zhou, Wei Li, and Peter J. Liu. Exploring the limits of transfer learning with a unified text-to-text transformer. *Journal of Machine Learning Research*, 21(140):1–67, 2020. URL <http://jmlr.org/papers/v21/20-074.html>.
- [70] Adam Roberts, Colin Raffel, and Noam Shazeer. How much knowledge can you pack into the parameters of a language model? *CoRR*, abs/2002.08910, 2020. URL <https://arxiv.org/abs/2002.08910>.
- [71] S. Sagawa, A. Raghunathan, P. W. Koh, and P. Liang. An investigation of why overparameterization exacerbates spurious correlations. In *International Conference on Machine Learning (ICML)*, 2020.
- [72] Victor Sanh, Lysandre Debut, Julien Chaumond, and Thomas Wolf. Distilbert, a distilled version of BERT: smaller, faster, cheaper and lighter. *CoRR*, abs/1910.01108, 2019. URL <http://arxiv.org/abs/1910.01108>.
- [73] Cory Stephenson, suchismita padhy, Abhinav Ganesh, Yue Hui, Hanlin Tang, and SueYeon Chung. On the geometry of generalization and memorization in deep neural networks. In *International Conference on Learning Representations*, 2021. URL <https://openreview.net/forum?id=V8jrrnwGbuc>.
- [74] Charles J. Stone. Consistent Nonparametric Regression. *The Annals of Statistics*, 5(4):595–620, 1977. doi: 10.1214/aos/1176343886. URL <https://doi.org/10.1214/aos/1176343886>.
- [75] Mariya Toneva, Alessandro Sordani, Remi Tachet des Combes, Adam Trischler, Yoshua Bengio, and Geoffrey J. Gordon. An empirical study of example forgetting during deep neural network learning. In *7th International Conference on Learning Representations, ICLR 2019, New Orleans, LA, USA, May 6-9, 2019*. OpenReview.net, 2019. URL <https://openreview.net/forum?id=BJLxm30cKm>.
- [76] Vladimir Vapnik and Rauf Izmailov. Reinforced SVM method and memorization mechanisms. *Pattern Recognition*, 119:108018, 2021. ISSN 0031-3203. doi: <https://doi.org/10.1016/j.patcog.2021.108018>. URL <https://www.sciencedirect.com/science/article/pii/S0031320321002053>.
- [77] Ke Wang, Vidya Muthukumar, and Christos Thrampoulidis. Benign overfitting in multiclass classification: All roads lead to interpolation, 2021. URL <https://arxiv.org/abs/2106.10865>.
- [78] Zhen Wang and Yuan-Hai Shao. Generalization-memorization machines, 2022. URL <https://arxiv.org/abs/2207.03976>.
- [79] Jiaheng Wei, Zhaowei Zhu, Hao Cheng, Tongliang Liu, Gang Niu, and Yang Liu. Learning with noisy labels revisited: A study using real-world human annotations. In *International Conference on Learning Representations*, 2022. URL <https://openreview.net/forum?id=TBWA6PLJZQm>.
- [80] Han Xu, Xiaorui Liu, Wentao Wang, Zitao Liu, Anil K. Jain, and Jiliang Tang. How does the memorization of neural networks impact adversarial robust models? In *Proceedings of the 29th ACM SIGKDD Conference on Knowledge Discovery and Data Mining, KDD*, 2023.

- [81] Zitong Yang, Michal Lukasik, Vaishnavh Nagarajan, Zonglin Li, Ankit Singh Rawat, Manzil Zaheer, Aditya Krishna Menon, and Sanjiv Kumar. Resmem: Learn what you can and memorize the rest, 2023.
- [82] Quanming Yao, Hansi Yang, Bo Han, Gang Niu, and James Tin-Yau Kwok. Searching to exploit memorization effect in learning with noisy labels. In Hal Daumé III and Aarti Singh, editors, *Proceedings of the 37th International Conference on Machine Learning*, volume 119 of *Proceedings of Machine Learning Research*, pages 10789–10798. PMLR, 13–18 Jul 2020. URL <https://proceedings.mlr.press/v119/yao20b.html>.
- [83] Chiyuan Zhang, Samy Bengio, Moritz Hardt, Benjamin Recht, and Oriol Vinyals. Understanding deep learning requires rethinking generalization. In *5th International Conference on Learning Representations, ICLR 2017, Toulon, France, April 24-26, 2017, Conference Track Proceedings*. OpenReview.net, 2017.
- [84] Chiyuan Zhang, Samy Bengio, Moritz Hardt, Michael C. Mozer, and Yoram Singer. Identity crisis: Memorization and generalization under extreme overparameterization. In *International Conference on Learning Representations*, 2020. URL <https://openreview.net/forum?id=B1l6y0VFPPr>.
- [85] Chiyuan Zhang, Daphne Ippolito, Katherine Lee, Matthew Jagielski, Florian Tramèr, and Nicholas Carlini. Counterfactual memorization in neural language models. *CoRR*, abs/2112.12938, 2021. URL <https://arxiv.org/abs/2112.12938>.
- [86] Xiaosen Zheng and Jing Jiang. An empirical study of memorization in NLP. In *Proceedings of the 60th Annual Meeting of the Association for Computational Linguistics (Volume 1: Long Papers)*, pages 6265–6278, Dublin, Ireland, May 2022. Association for Computational Linguistics. doi: 10.18653/v1/2022.acl-long.434. URL <https://aclanthology.org/2022.acl-long.434>.
- [87] Chunting Zhou, Jiatao Gu, and Graham Neubig. Understanding knowledge distillation in non-autoregressive machine translation. In *International Conference on Learning Representations*, 2020. URL <https://openreview.net/forum?id=BygFVAEKDH>.
- [88] Hattie Zhou, Ankit Vani, Hugo Larochelle, and Aaron Courville. Fortuitous forgetting in connectionist networks. In *International Conference on Learning Representations*, 2022. URL https://openreview.net/forum?id=ei3SY1_zYsE.

Appendix

Table of Contents

A	Limitations	19
B	Societal impact	19
C	Broader impact	19
D	Hyperparameter settings	20
E	Summary of train and test performance with model depth	21
F	Additional experiments: memorisation score distributions	22
F.1	Memorisation score distributions across datasets	22
F.2	Memorisation score distributions for varying ResNet width	22
F.3	Memorisation score distribution under distillation	22
G	Additional experiments: larger models memorise some samples <i>more</i>	25
H	Additional experiments and discussion: per-example memorisation trajectories	26
H.1	An intuition behind the categorisations.	26
H.2	On predicted labels and memorisation trajectories	26
H.3	An intuition for why memorisation (mostly) lowers with depth	36
H.4	Memorisation trajectories under distillation	38
H.5	Memorisation trajectories on ImageNet	40
I	Memorisation and robustness	45
J	Additional experiments: prediction depth and cprox	46
J.1	On the choice of probes for prediction depth	46
J.2	Per-sample score trajectories	46

A Limitations

We identify the following limitations of our work:

- While elegant and established as the memorisation score, the metric for memorisation we use (as defined in Equation 1), even with the approximation we use (as shown in Equation 2) is expensive to compute as it requires training of many models. We consider finding an efficient and faithful proxy to memorisation score to be an important future work direction.
- We conduct experiments in the image classification domain. While we do experiment on multiple datasets (CIFAR-100, CIFAR-10, ImageNet, TinyImagenet) and model architectures (ResNet, MobileNet, LeNet), it would be of interest to analyse whether similar trends will be observed in NLP tasks.

B Societal impact

We highlight some points regarding the societal impact of our work below:

1. Understanding memorisation is important as it can manifest in undesired behavior by the underlying model. This becomes more critical given that ML models are increasingly being utilized in various areas that affect human life.
2. Even though we have provided a detailed study of model memorization on standard benchmarks, a domain specific exploration is needed for individual models before they are deployed in practice.
3. As pointed out by our study, the memorisation behaviour of a model is tied to noise in the dataset. Thus, our work emphasizes the need for ensuring data quality.
4. Finally, our memorization study requires training multiple models which leads to a negative environmental impact. But we hope that the insights from our findings can in the long term serve as guiding principles for future studies and reduce computation in future.

C Broader impact

Our work has multiple implications and future work directions.

First, we would like to emphasise the importance of our findings for the broader goal of developing a better understanding of deep learning. Both the increasing bi-modality of memorisation scores with increasing model capacity, and the existence of a variety of trajectories of memorisation scores with increasing model capacity, are to our knowledge new observations in the community. The question of why distillation improves generalisation is still under study by the community. Our work contributes to this branch of work by studying memorisation under distillation.

Next, we identify that the following practical implications can be drawn from our work:

Our study leads to an important practical conclusion that one should be careful with using certain statistics as proxies for memorisation. Previous works suggested that certain statistics based on model training or model inference (which we discuss in Section 5) can provide efficient proxies for memorisation score. Although these proxies appear to yield high correlation to memorisation, we find that distributionally they are significantly different, and do not capture the key aspects of memorization score that we uncover. This points at a future direction of identifying better memorisation score proxies which could be efficiently computed.

Our study points to a potentially sound way for identifying noisy examples in the labelled data. Specifically, we find the existence of examples with increasing memorisation over model capacity even after interpolation. We qualitatively find that they are often ambiguous and mislabeled. For example, one general conclusion from this is that if the average memorisation of a subset of train data grows with model capacity, this can point at a possibility of poor quality of the labels in that set.

Our study points at a potential application of weighting examples based on memorisation score during distillation. Improving distillation by reweighting or filtering examples is an active research direction in the community. Given the finding how distillation lowers the memorisation of train examples, and how interestingly this is often achieved by lowering the interpolation (as we show in Figure 5), this suggests that memorisation could be used for improving memorisation by filtering out or downweighting examples which the model ends up memorising.

D Hyperparameter settings

Our experiments use standard ResNet-v2 [37] and MobileNet-v3 [43] architectures. Specifically, for CIFAR, we consider the CIFAR ResNet- $\{110, 56, 44, 32, 20, 14, 8\}$ family of architectures; for Tiny-ImageNet, we consider the ResNet- $\{152, 101, 50, 34, 18\}$ and the MobileNet-v3 Large architecture with scale factors $\{0.35, 0.50, 0.75, 1.00, 1.25\}$. For all ResNet models, we employ standard augmentations as per He et al. [38].

We train all models to minimise the softmax cross-entropy loss via minibatch SGD, with hyperparameter settings per Table 4.

Parameter	CIFAR-10*	Tiny-ImageNet
Weight decay	10^{-4}	$5 \cdot 10^{-4}$
Batch size	1024	256
Epochs	450	90
Peak learning rate	1.0	0.1
Learning rate warmup epochs	15	5
Learning rate decay factor	0.1	Cosine schedule
Learning rate decay epochs	200, 300, 400	N/A
Nesterov momentum	0.9	0.9
Distillation weight	1.0	1.0
Distillation temperature	3.0	1.0

Table 4: Summary of training hyperparameter settings.

E Summary of train and test performance with model depth

In Table 5 we report train and test accuracies across architectures on CIFAR-100 from the one-hot training, while in Table 6 we report train and test accuracies from the distillation training across teachers of varying depths. We find that increasing depth results in models that *interpolate* the training set, while also generalising better on the test set. We also show how distillation worsens train accuracy while improving the test accuracy.

Architecture	Train	Test
ResNet-8	0.66	0.57
ResNet-14	0.82	0.65
ResNet-20	0.90	0.67
ResNet-32	0.98	0.69
ResNet-44	1.00	0.71
ResNet-56	1.00	0.71
ResNet-110	1.00	0.73

Table 5: Train and test accuracies across architectures on CIFAR-100. Consistent with a growing body of work, on the clean dataset we find that increasing depth results in models that *interpolate* the training set, while also generalising better on the test set.

(a) ResNet-110 teacher.			(b) ResNet-56 teacher.		
Architecture	Train	Test	Architecture	Train	Test
ResNet-110→ResNet-8	0.65	0.59	ResNet-56→ResNet-8	0.67	0.60
ResNet-110→ResNet-14	0.68	0.58	ResNet-56→ResNet-14	0.81	0.69
ResNet-110→ResNet-20	0.78	0.64	ResNet-56→ResNet-20	0.88	0.71
ResNet-110→ResNet-32	0.95	0.73	ResNet-56→ResNet-32	0.94	0.74
ResNet-110→ResNet-44	0.98	0.74	ResNet-56→ResNet-44	0.97	0.75
ResNet-110→ResNet-56	0.99	0.75	ResNet-56→ResNet-56	0.98	0.75

Table 6: Train and test accuracies across architectures on CIFAR-100 under distillation averaged over 5 runs. We find that, compared to the model of corresponding architecture trained using the one-hot objective, distillation lowers train accuracy and in most cases improves test accuracy.

F Additional experiments: memorisation score distributions

F.1 Memorisation score distributions across datasets

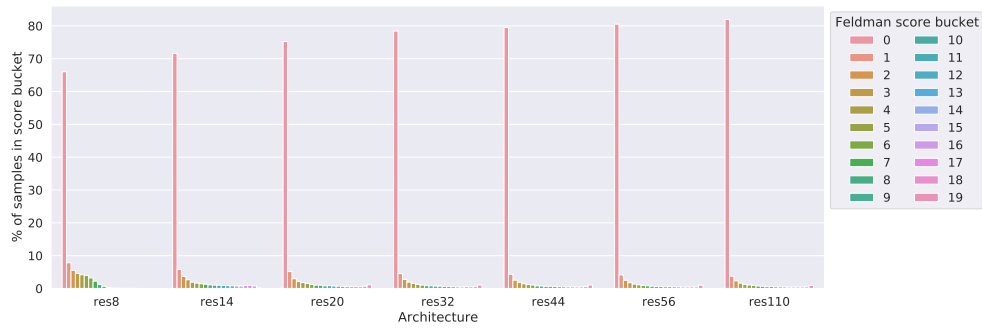
In Figure 6 we show the histogram of memorisation scores as a function of model depth. As in the body, we see that increasing depth has the effect of exaggerating the bi-modality of the scores.

F.2 Memorisation score distributions for varying ResNet width

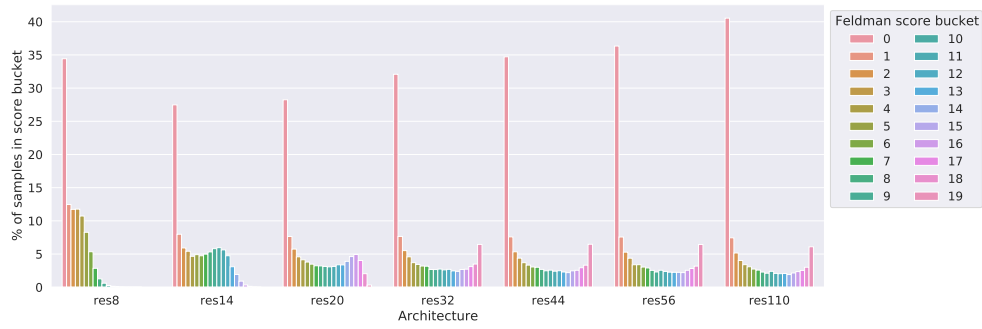
Figure 7 shows a similar plot on CIFAR-100, where we vary the *width* of a ResNet-32 model.

F.3 Memorisation score distribution under distillation

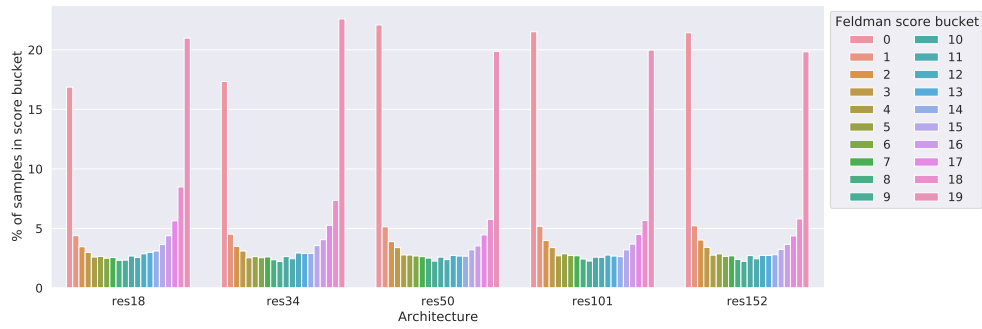
Figure 16 shows how memorisation distribution changes under distillation across architectures and datasets. Consistently with the one-hot training depicted in Figure 6 we see both the high memorisation and low memorisation points to increase in number as architecture becomes deeper.



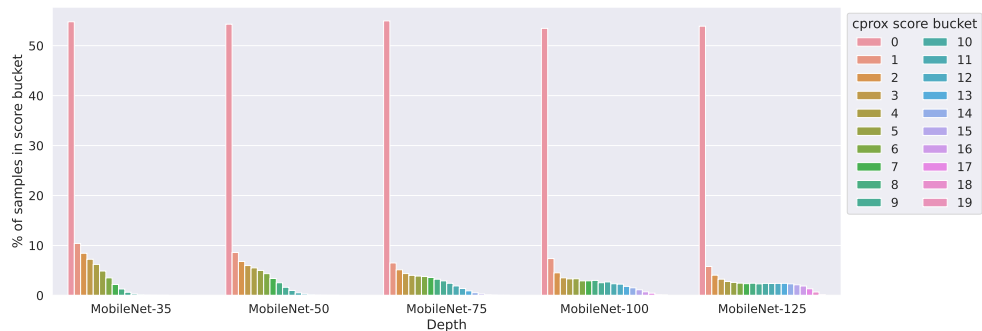
(a) CIFAR-10.



(b) CIFAR-100.



(c) Tiny ImageNet.



(d) ImageNet.

Figure 6: Distributions of memorisation scores across datasets and model sizes. A general trend is that the memorisation scores are *bi-modal* (for sufficiently large models), with most samples’ score being close to 0 or 1. Further, this bi-modality is *exaggerated with model depth*: larger models (unsurprisingly) assign low score (“generalise”) on relatively more samples, *but* also (more surprisingly) assign high score (“memorise”) on relatively more samples as well.



Figure 7: Distributions of memorisation scores across model *widths* of a ResNet-32 on CIFAR-100. A general trend is that the memorisation scores are *bi-modal*, with most samples’ score being close to 0 or 1. Further, this bi-modality is *exaggerated with model width*: larger models (unsurprisingly) assign low score (“generalise”) on relatively more samples, *but* also (more surprisingly) assign high score (“memorise”) on relatively more samples as well.

G Additional experiments: larger models memorise some samples *more*

Given the observation of the increasing bi-modality with model depth, we now study how exactly the memorisation score of each example shifts across model depths. In Figure 8, we show how memorisation scores evolve with depth on a *per-example* basis. An unsurprising observation is that memorisation scores in most cases do not significantly change across depths. Beyond this, we can see that as the difference in depths becomes larger, the highly memorised examples according to a small model become *less* memorised by the large model (note the high density in the lower-right part of the plot).

Most interestingly, in all cases, there is a non-trivial fraction of samples whose memorisation score *increases* with model size: note the horizontal bar at the top of multiple subfigures in Figure 8. Increasing memorisation implies a *decreasing* out-of-sample accuracy on such points (as the in-sample accuracy monotonically increases with model depth). This is perhaps surprising, since one expects increasing model depth to improve generalisation [61].

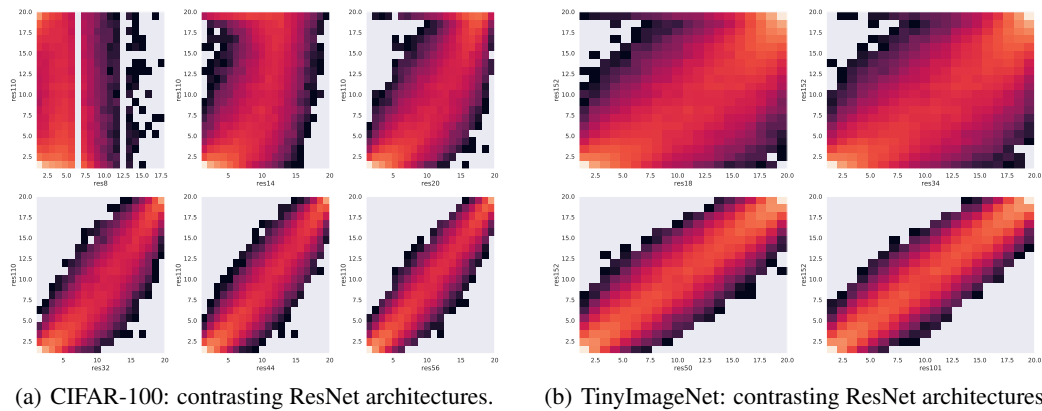


Figure 8: Contrasting per-example memorisation scores across architectures in different setups. As the difference in depths becomes larger, the highly memorised examples according to a small model become *less* memorised by the large model (note the high density in the lower-right part of the plot). On the other hand, smaller models tend to have examples which get assigned a high memorisation score by a large model (note the horizontal bar at the top of a figure).

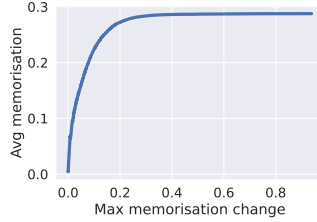


Figure 9: Average memorisation on CIFAR-100 examples where memorisation changes by at most x . Least changing examples are less memorised.

H Additional experiments and discussion: per-example memorisation trajectories

H.1 An intuition behind the categorisations.

The categorisations we introduce can be intuitively explained by breaking down the *Feldman memorisation* score into in-sample and out-of-sample accuracy components. For the examples which are easy across model depths, we expect the in-sample and out-of-sample accuracy to be high, and so find a low and unchanging memorisation across depths. Next, for the hard but unambiguous examples, we expect out-of-sample accuracy for that example to be increasing, which corresponds to the gradually increasing generalisation, and in turn, the memorisation score decreasing after reaching the interpolation regime (i.e., where the in-sample accuracy is 100%). This corresponds to the cap-shaped and decreasing trajectories (the interpolation regime is reached even by the smaller models for the latter). Finally, for the mislabeled or ambiguous examples in the data, we find the *correct* label, which disagrees with the *noisy* or ambiguous label in the data, is being recovered better by the deeper models, and so the in-sample accuracy increases or remains high. This corresponds to a high or even increasing memorisation.

Interestingly, Wei et al. [79] find that noisy examples are eventually memorised by the model (here, memorisation was defined as the confidence in the ground truth label), however the *non-noisy* examples are fitted first. This parallels our observations about memorisation of noisy examples increasing, as the labels get interpolated, but the model does not generalise to the noisy labels.

H.2 On predicted labels and memorisation trajectories

In Figures 10 and 12 we show additional examples of per example trajectories. We focus on the following three categories: *least changing*, *most increasing* and *most decreasing or U-shaped* in memorisation as the model capacity increases. In Tables 7 and 8 we show predictions from ResNet-20 and ResNet-110 for each example depicted across the Figures. In the discussion below, we refer to examples from Figure 10.

We find that predictions for the *least changing* memorisation examples are saturated in the correct class, demonstrating that these are easy across model architectures. Predictions for the examples with *most decreasing or U-shaped* are assigned low probability from ResNet-20 for the correct class, and high probability from ResNet-110. We can see that these examples are often challenging and mislabeled by reasonable classes early on (e.g., the `bowl` example with a high probability for `clock` and `plate`).

Predictions for the examples with *most increasing* are often assigned high probability from ResNet-20 to categories which are also present in the image (`willow tree` also contains `forest`, and `telephone` also contains `keyboard`). We call these *hard labeled ambiguous examples*. The other type we can see are *ambiguous examples*, such as `shark` and `pear`, which are not clear and easily confused with other labels as predicted by ResNet-110 (respectively, `dolphin` and `sweet pepper` labels).

We believe the presence of ambiguous examples among both increasing and decreasing memorisation trajectories may be explained by the fact that the multiple labels of ambiguous points may contain labels of various difficulty, with the smaller models assigning high probability to the easy labels, while larger models shift more towards the harder labels. Then, depending on whether the easy or the hard

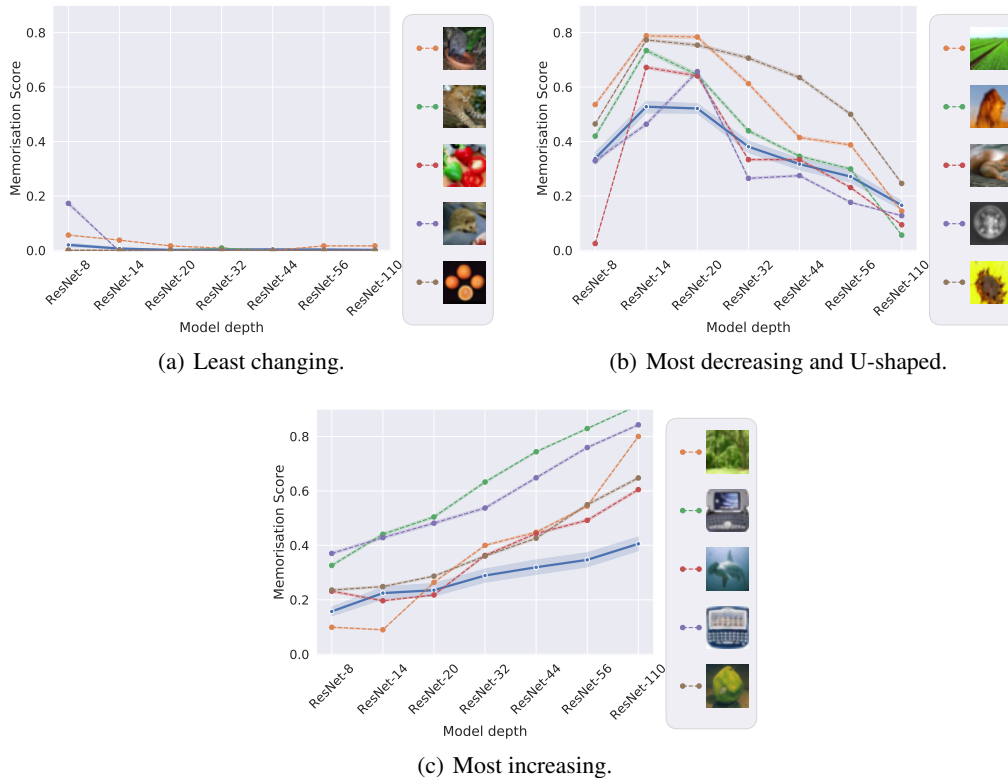


Figure 10: Memorisation of examples across model depths which are interpolated by a ResNet-20 model, and trajectories of memorisation for examples with: the change in memorisation closest to zero, the most decreasing memorisation, and the most increasing memorisation, when comparing ResNet-20 and ResNet-110 architectures. Solid blue line denotes average trajectory according to the top 1% example selected based on the corresponding criterion, and the dashed lines denote top 5 examples according to the corresponding criterion. We find that the fixed memorisation examples are easy and unambiguous, as is the case for porcupine. The decreasing memorisation example (plain) is arguably more complex and gets confused with caterpillar and road classes by ResNet-20. The increasing memorisation example (willow tree) is ambiguous (ResNet-110 predicts forest which is arguably also a valid label). In Table 7, we show predictions from ResNet-20 and ResNet-110 for each example depicted across the subfigures.

label is present in the training set, different memorization trajectories are observed. If the observed label is the easier label, as model size gets larger, more probability gets assigned to the harder labels. Thus, increasing model size may lead to increasing memorisation trajectory. Conversely, if the observed label is the harder label, increasing model size may lead to the decreasing memorisation trajectory.

We note that previous works offered different metrics for identifying difficult examples, with a prominent example of categorisation according to prediction depth [5]. We can compare Figure 1 with Figure 28 to see whether the categorisation by memorisation trajectories can be recovered with prediction depth. We see how the most and the least changing examples in terms of their memorisation score are not clearly distinguished when considering prediction depth: most of them get assigned a very high prediction depth scores across architectures.

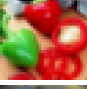
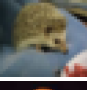

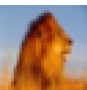





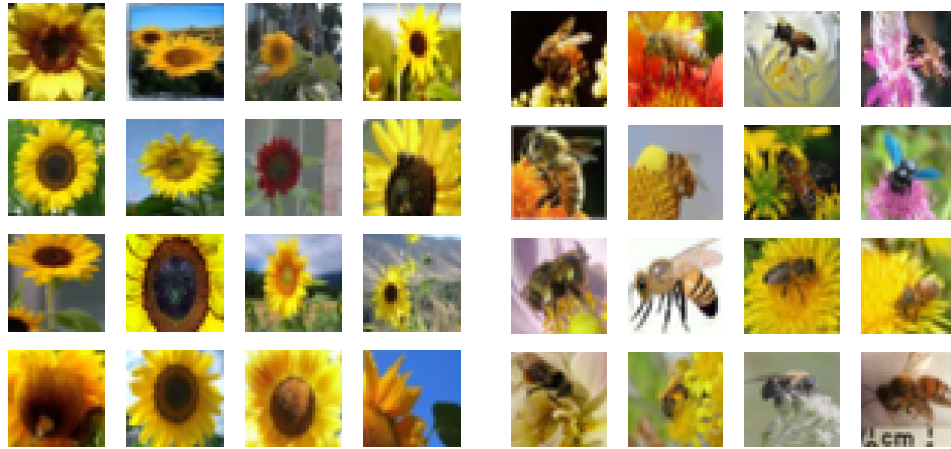
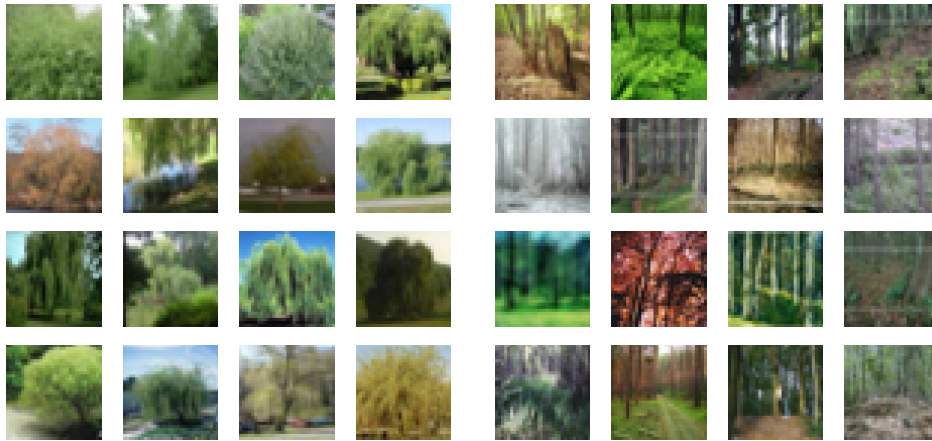
Example	Label	ResNet-20 predictions	ResNet-110 predictions
	porcupine	porcupine: 0.98 crab: 0.01 possum: 0.01	porcupine: 0.98 shrew: 0.02 girl: 0.00
	leopard	leopard: 1.00 worm: 0.00 hamster: 0.00	leopard: 1.00 worm: 0.00 hamster: 0.00
	sweet pepper	sweet pepper: 1.00 worm: 0.00 girl: 0.00	sweet pepper: 1.00 worm: 0.00 girl: 0.00
	porcupine	porcupine: 1.00 worm: 0.00 girl: 0.00	porcupine: 1.00 worm: 0.00 girl: 0.00
	orange	orange: 1.00 worm: 0.00 hamster: 0.00	orange: 1.00 worm: 0.00 hamster: 0.00
	plain	caterpillar: 0.39 plain: 0.22 worm: 0.20	plain: 0.86 caterpillar: 0.08 road: 0.02
	lion	lion: 0.36 camel: 0.16 skyscraper: 0.09	lion: 0.94 skyscraper: 0.02 hamster: 0.01
	squirrel	squirrel: 0.36 snail: 0.27 seal: 0.21	squirrel: 0.91 snail: 0.06 seal: 0.03
	bowl	bowl: 0.34 clock: 0.29 plate: 0.15	bowl: 0.87 plate: 0.06 clock: 0.03
	sunflower	bee: 0.30 sunflower: 0.25 butterfly: 0.20	sunflower: 0.75 bee: 0.10 butterfly: 0.06
	willow tree	willow tree: 0.74 forest: 0.21 palm tree: 0.03	forest: 0.75 willow tree: 0.20 oak tree: 0.02
	telephone	telephone: 0.50 television: 0.40 keyboard: 0.06	television: 0.88 telephone: 0.09 keyboard: 0.03
	shark	shark: 0.78 dolphin: 0.15 whale: 0.05	shark: 0.40 dolphin: 0.32 whale: 0.21
	telephone	telephone: 0.52 keyboard: 0.37 clock: 0.08	keyboard: 0.74 telephone: 0.16 clock: 0.09
	pear	pear: 0.71 sweet pepper: 0.21 aquarium fish: 0.03	sweet pepper: 0.45 pear: 0.35 bowl: 0.12

Table 7: Predictions from ResNet-20 and ResNet-110 for each example depicted in Figure 10.



(a) Sunflower class examples.

(b) Bee class examples.



(c) Willow tree class examples.

(d) Forest class examples.

Figure 11: Randomly chosen examples from four classes from CIFAR-100 dataset: sunflower, bee, willow tree and forest.

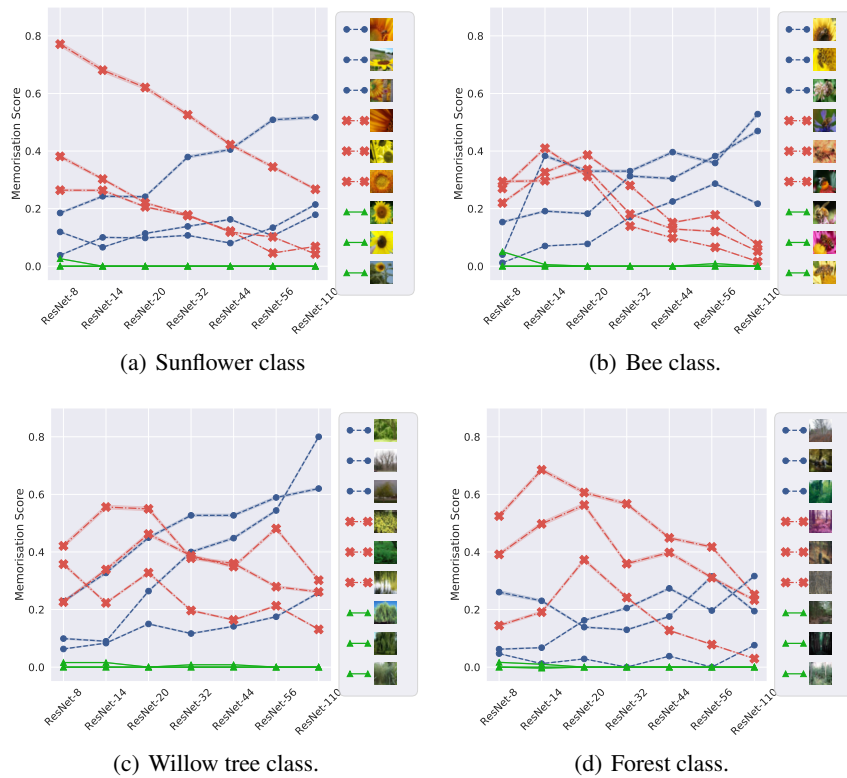


Figure 12: Memorisation of examples from a specific label across model depths which are interpolated by a ResNet-20 model, and trajectories of memorisation for examples with: the change in memorisation closest to zero, the most decreasing memorisation, and the most increasing memorisation, when comparing ResNet-20 and ResNet-110 architectures.

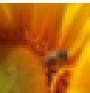








Example	Label	ResNet-20 predictions	ResNet-110 predictions
	sunflower	sunflower: 0.76 bee: 0.18 poppy: 0.05	sunflower: 0.48 bee: 0.45 poppy: 0.06
	sunflower	television: 0.75 wardrobe: 0.11 can: 0.08	television: 0.71 wardrobe: 0.12 tiger: 0.10
	sunflower	willow tree: 0.29 forest: 0.27 maple tree: 0.22	willow tree: 0.53 forest: 0.41 maple tree: 0.05
	sunflower	sunflower: 0.38 sweet pepper: 0.20 rose: 0.06	sunflower: 0.73 sweet pepper: 0.09 pear: 0.03
	sunflower	sunflower: 0.71 lobster: 0.14 crab: 0.10	sunflower: 1.00 worm: 0.00 girl: 0.00
	sunflower	sunflower: 0.70 bicycle: 0.07 spider: 0.05	sunflower: 0.96 bicycle: 0.02 man: 0.01
	sunflower	sunflower: 1.00 worm: 0.00 girl: 0.00	sunflower: 1.00 worm: 0.00 girl: 0.00
	sunflower	sunflower: 1.00 worm: 0.00 girl: 0.00	sunflower: 1.00 worm: 0.00 girl: 0.00
	sunflower	sunflower: 1.00 worm: 0.00 girl: 0.00	sunflower: 1.00 worm: 0.00 girl: 0.00

Table 8: Predictions from ResNet-20 and ResNet-110 for each example from Figure 12.


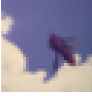

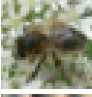
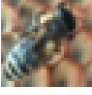

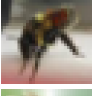
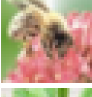

Example	Label	ResNet-20 predictions	ResNet-110 predictions
	bee	mouse: 0.31 squirrel: 0.17 possum: 0.14	mouse: 0.44 squirrel: 0.27 rabbit: 0.08
	bee	rocket: 0.56 lizard: 0.11 cloud: 0.09	rocket: 0.44 cloud: 0.21 lizard: 0.09
	bee	lamp: 0.25 can: 0.23 telephone: 0.19	can: 0.36 telephone: 0.25 lamp: 0.17
	bee	bee: 0.70 shrew: 0.15 beetle: 0.05	bee: 1.00 worm: 0.00 house: 0.00
	bee	bee: 0.71 wolf: 0.05 tiger: 0.04	bee: 0.95 wolf: 0.01 shrew: 0.01
	bee	bee: 0.74 crab: 0.10 beetle: 0.06	bee: 0.95 cockroach: 0.03 beetle: 0.02
	bee	bee: 1.00 worm: 0.00 house: 0.00	bee: 1.00 worm: 0.00 house: 0.00
	bee	bee: 1.00 worm: 0.00 house: 0.00	bee: 1.00 worm: 0.00 house: 0.00
	bee	bee: 0.98 caterpillar: 0.01 squirrel: 0.01	bee: 0.98 caterpillar: 0.02 worm: 0.00

Table 9: Predictions from ResNet-20 and ResNet-110 for each example from Figure 12.




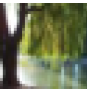

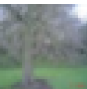

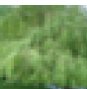
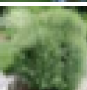
Example	Label	ResNet-20 predictions	ResNet-110 predictions
	willow tree	oak tree: 0.65 maple tree: 0.34 pine tree: 0.01	oak tree: 0.64 maple tree: 0.35 pine tree: 0.01
	willow tree	oak tree: 0.67 maple tree: 0.32 pine tree: 0.01	oak tree: 0.87 maple tree: 0.13 hamster: 0.00
	willow tree	oak tree: 0.37 maple tree: 0.36 pine tree: 0.27	oak tree: 0.41 maple tree: 0.35 pine tree: 0.24
	willow tree	willow tree: 0.81 forest: 0.12 pear: 0.02	willow tree: 0.95 forest: 0.04 bottle: 0.01
	willow tree	willow tree: 0.46 sunflower: 0.16 forest: 0.16	willow tree: 0.61 forest: 0.32 caterpillar: 0.03
	willow tree	willow tree: 0.81 forest: 0.10 pine tree: 0.05	willow tree: 0.94 forest: 0.05 cloud: 0.01
	willow tree	willow tree: 0.98 forest: 0.02 worm: 0.00	willow tree: 0.98 forest: 0.02 worm: 0.00
	willow tree	willow tree: 1.00 worm: 0.00 hamster: 0.00	willow tree: 1.00 worm: 0.00 hamster: 0.00
	willow tree	willow tree: 1.00 worm: 0.00 hamster: 0.00	willow tree: 1.00 worm: 0.00 hamster: 0.00

Table 10: Predictions from ResNet-20 and ResNet-110 for each example from Figure 12.



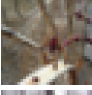
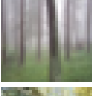
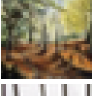



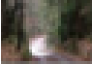
Example	Label	ResNet-20 predictions	ResNet-110 predictions
	forest	road: 1.00 worm: 0.00 girl: 0.00	road: 1.00 worm: 0.00 girl: 0.00
	forest	train: 0.76 streetcar: 0.18 pine tree: 0.02	train: 0.82 streetcar: 0.16 tank: 0.02
	forest	spider: 0.32 lizard: 0.21 dinosaur: 0.13	spider: 0.51 lobster: 0.17 table: 0.12
	forest	forest: 0.80 wardrobe: 0.11 skyscraper: 0.02	forest: 0.98 wardrobe: 0.02 worm: 0.00
	forest	forest: 0.86 dinosaur: 0.04 crab: 0.02	forest: 0.98 bridge: 0.01 tractor: 0.01
	forest	forest: 0.90 bridge: 0.03 house: 0.03	forest: 0.99 table: 0.01 worm: 0.00
	forest	forest: 1.00 worm: 0.00 hamster: 0.00	forest: 1.00 worm: 0.00 hamster: 0.00
	forest	forest: 1.00 worm: 0.00 hamster: 0.00	forest: 1.00 worm: 0.00 hamster: 0.00
	forest	forest: 1.00 worm: 0.00 hamster: 0.00	forest: 1.00 worm: 0.00 hamster: 0.00

Table 11: Predictions from ResNet-20 and ResNet-110 for each example from Figure 12.



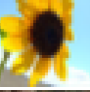
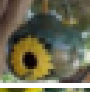
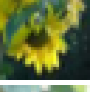
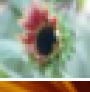
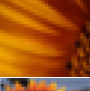

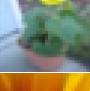
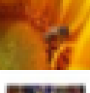
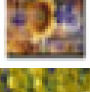

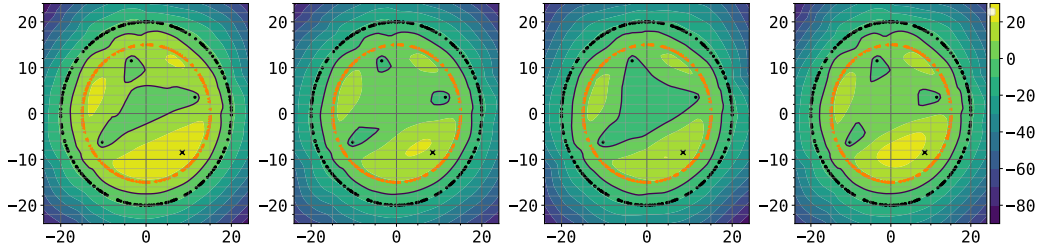
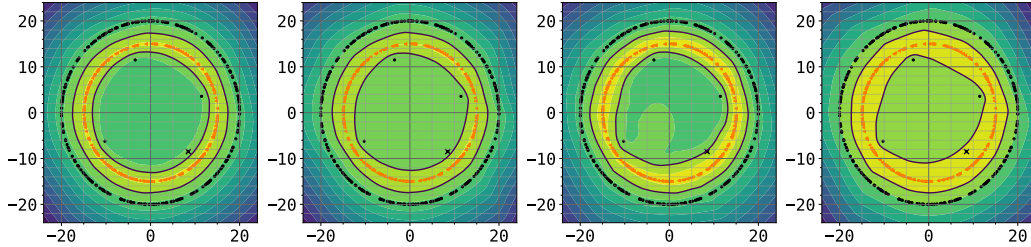
Example	Label	ResNet-20 predictions	ResNet-110 predictions
	sunflower	sunflower: 1.00 worm: 0.00 girl: 0.00	sunflower: 1.00 worm: 0.00 girl: 0.00
	sunflower	sunflower: 1.00 worm: 0.00 girl: 0.00	sunflower: 1.00 worm: 0.00 girl: 0.00
	sunflower	sunflower: 1.00 worm: 0.00 girl: 0.00	sunflower: 1.00 worm: 0.00 girl: 0.00
	sunflower	bowl: 0.36 sunflower: 0.15 snake: 0.08	sunflower: 0.61 bowl: 0.11 ray: 0.07
	sunflower	sunflower: 0.84 orchid: 0.08 poppy: 0.02	sunflower: 0.95 orchid: 0.02 butterfly: 0.01
	sunflower	bee: 0.29 poppy: 0.16 sunflower: 0.15	sunflower: 0.50 bee: 0.26 poppy: 0.12
	sunflower	sunflower: 0.38 sweet pepper: 0.20 rose: 0.06	sunflower: 0.73 sweet pepper: 0.09 pear: 0.03
	sunflower	sunflower: 0.71 lobster: 0.14 crab: 0.10	sunflower: 1.00 worm: 0.00 girl: 0.00
	sunflower	sunflower: 0.78 bowl: 0.09 poppy: 0.07	sunflower: 0.97 sweet pepper: 0.03 worm: 0.00
	sunflower	sunflower: 0.76 bee: 0.18 poppy: 0.05	sunflower: 0.48 bee: 0.45 poppy: 0.06
	sunflower	television: 0.75 wardrobe: 0.11 can: 0.08	television: 0.71 wardrobe: 0.12 tiger: 0.10
	sunflower	willow tree: 0.29 forest: 0.27 maple tree: 0.22	willow tree: 0.53 forest: 0.41 maple tree: 0.05

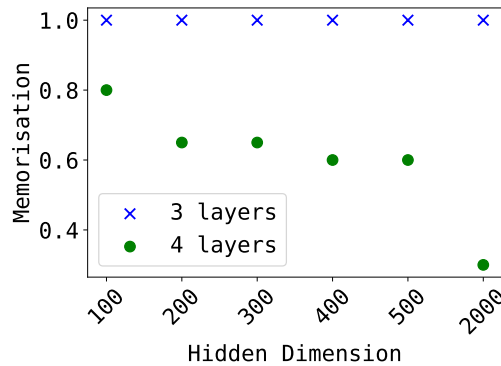
Table 12: Predictions from ResNet-20 and ResNet-110 for each example from Figure 1.



(a) Smaller model trained with different random seeds.



(b) Larger model trained with different random seeds.



(c) Memorisation score trajectory for the outlier example.

Figure 13: An illustration of an intuition for why larger models on average yield lower memorisation. We consider a 2D binary classification task where one class is distributed as a single circle (in red-orange), and the other class (in black) is distributed as an exterior circle along with a handful of “outlier” points inside the innermost circle. We visualize the decision boundary (the continuous black lines) when training a smaller model (1 hidden layer model with 10k dimensions; first row) and a larger model (4 hidden layers with 500 dimensions; second row) across multiple random seeds on this task, when *excluding* one of outliers (denoted by the black cross in the bottom-right of the innermost set of points). We observe that the larger model learns decision boundaries that form one contiguous region around the outliers; in contrast, the smaller model learned disconnected decision boundaries around these outliers. This means that for the larger model, out-of-sample accuracy for the excluded outlier is higher; in turn, the memorisation score would be lower. Indeed in the last row, we show the memorisation score for the highlighted example across models with different depths and hidden dimensions. As the model size increases, the memorisation score decreases. This hints that with increasing model capacity, one can expect smoother, contiguous regions learnt by a model and thus lower memorisation of samples.

H.3 An intuition for why memorisation (mostly) lowers with depth

We have seen that increasing model capacity tends to lower memorisation on average. We have also discussed an intuition behind how this phenomenon is based on the *in-sample accuracy* and the

out-of-sample accuracy. We next demonstrate a more concrete intuition on a synthetic example for why we expect that should be the case.

We consider a two-dimensional toy binary classification dataset with two classes denoted by black points (class 0) and orange points (class 1), in the form of concentric circles. We construct class 0 in a way that it has a few “outlier” points which are harder to generalize from — here, they are a handful points from an innermost circle in the distribution. In Figure 13, we visualise the decision regions learned by two models of different sizes: a smaller 1 hidden layer model with 10000 dimensions and a larger 4 hidden layers with 500 dimensions. In particular, we visualise the boundaries across multiple random seeds when *excluding* one of the outliers (denoted by the black cross). Concretely, we show the difference between logits returned by the model for the two classes; large positive (negative) values denote areas where the model is confident about the class being positive (negative). The decision boundary (where the logit difference is precisely zero) is denoted in a solid black line.

We observe that the large model learns smooth decision regions, with the inner circle being connected, as opposed to the disconnected areas learnt by the small model. At the same time, when calculating the stability-based memorisation score for the highlighted example, as model size increases, the memorisation score decreases (see Figure 13(c)). This hints that with increasing model capacity, one can expect the model to learn smoother and more contiguous regions; this can lead to better out-of-sample accuracy, and thus lower the memorisation of samples. In I (Appendix) we study a connection of memorisation to robustness using the same illustrative example.

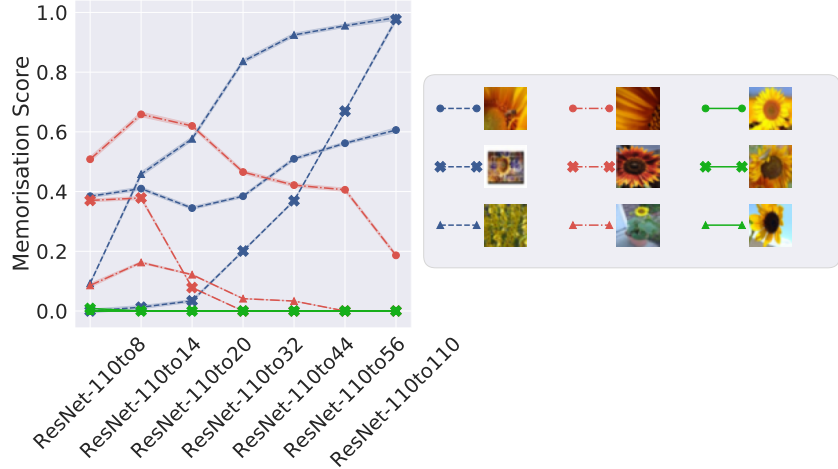


Figure 14: Illustration of how distillation affects how memorisation (in the sense of Equation 1) evolves with ResNet model depth on CIFAR-100 for examples depicted in Figure 1. We find that memorisation is overall lowered for the challenging and ambiguous examples.

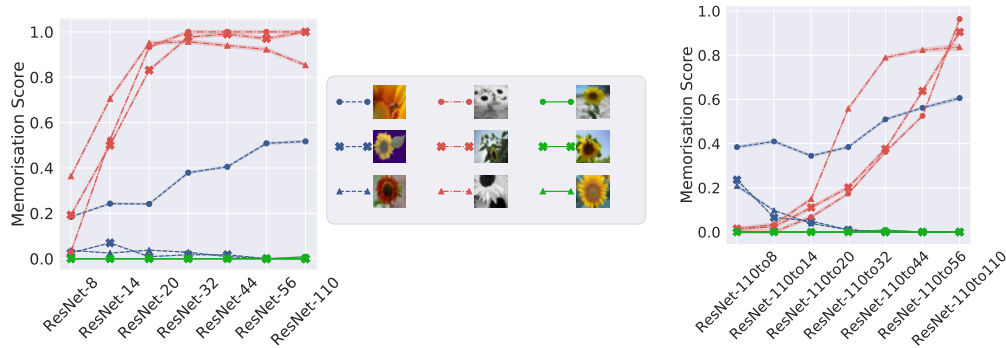


Figure 15: Evolution of memorisation score across one-hot (left) and distilled (right) models for examples across groups: where memorisation is most *increased* by distillation (blue), most *decreased* by distillation (red), and where it *least changes* (green). Distillation reduces memorisation most for hard and ambiguous examples. The remaining groups of examples are easy and unambiguous. A version of this Figure with standard deviations is shown in Figure 19.

H.4 Memorisation trajectories under distillation

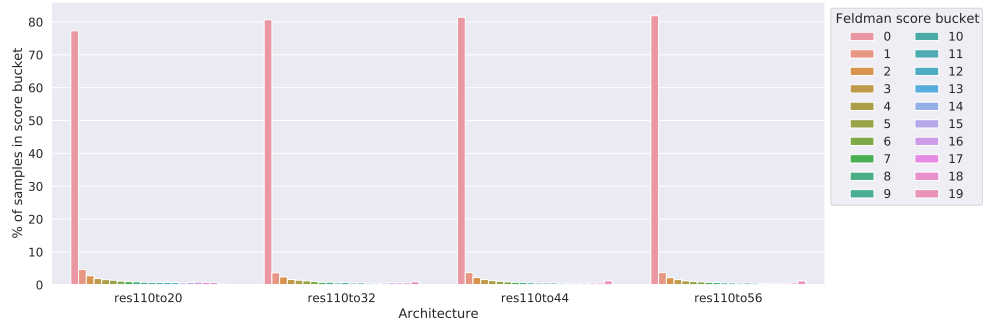
In Figure 14, we plot trajectories of memorisation under distillation for examples depicted in Figure 1. We find that memorisation is overall lowered for the challenging and ambiguous examples.

In Figure 16 we report distributions of memorisation under KD. We find that distillation preserves the increasing bimodality of the scores as the student architecture increases.

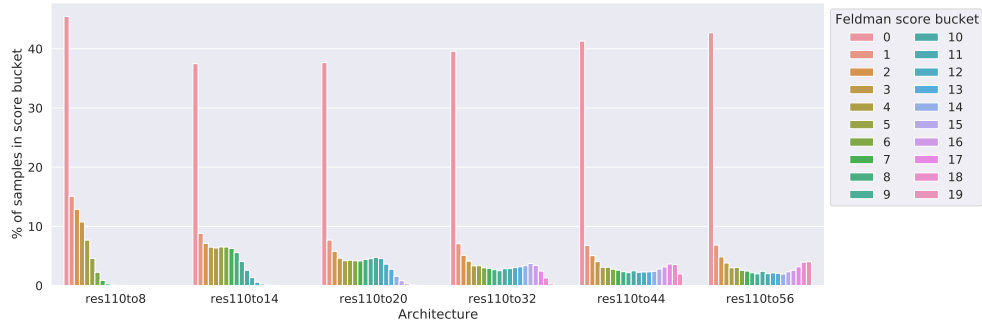
In Figure 17 we report additional results for how the memorisation scores change under distillation. We confirm the observations from 1(b) that distillation inhibits memorisation, especially for the highly memorised examples.

Figure 18 studies the effect of varying the teacher model used for distillation. Interestingly, the choice of teacher does not have a strong influence on the results, with even the self-distillation setting for a ResNet-32 resulting in an inhibition of memorisation.

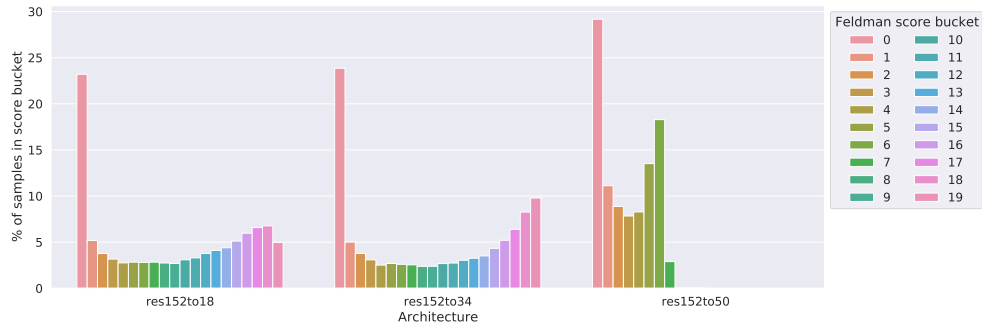
Figure 19 shows the evolution of memorisation scores for examples where memorisation is most increased, most decreased by distillation, and where it least changes. We find how the distillation least affects the memorisation of easy or unambiguous examples.



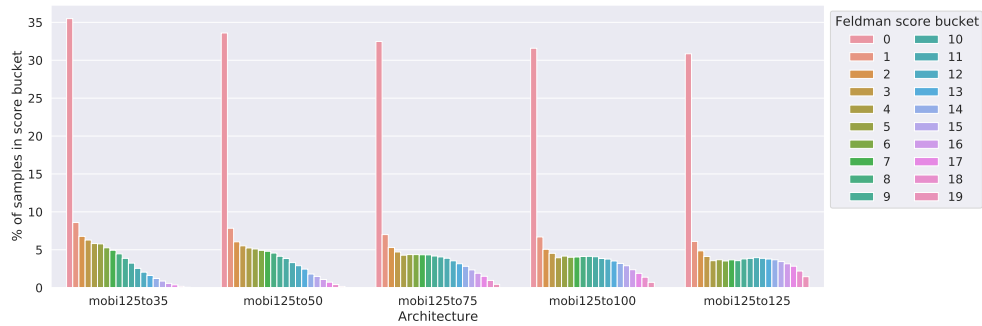
(a) CIFAR-10.



(b) CIFAR-100.



(c) Tiny ImageNet ResNet.



(d) Tiny ImageNet MobileNet.

Figure 16: Distributions of memorisation scores under knowledge distillation across datasets (different subfigures) and architectures (different bar colors in each subfigure). Similarly as under one-hot training, memorisation scores are *bi-modal*, and this bi-modality is *exaggerated with model depth*.

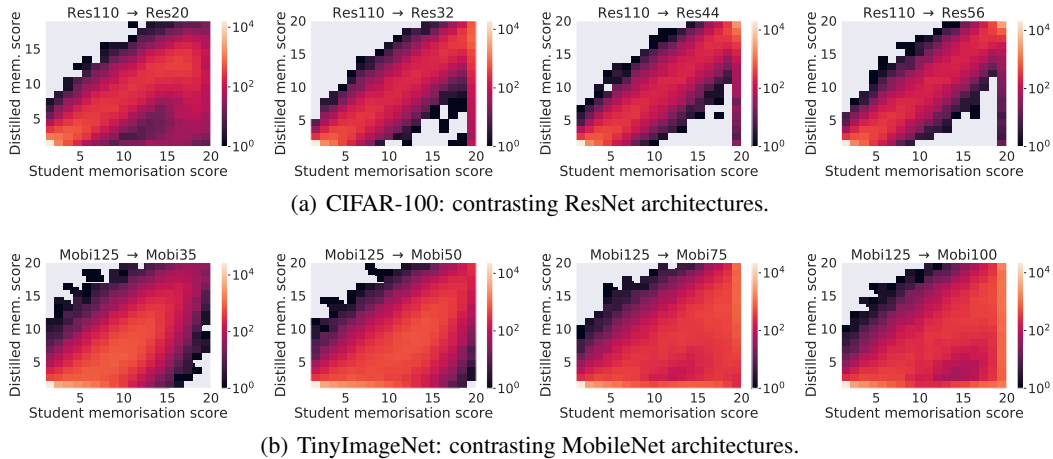


Figure 17: Contrasting per-example memorisation scores across distilled and one-hot student models in different setups.

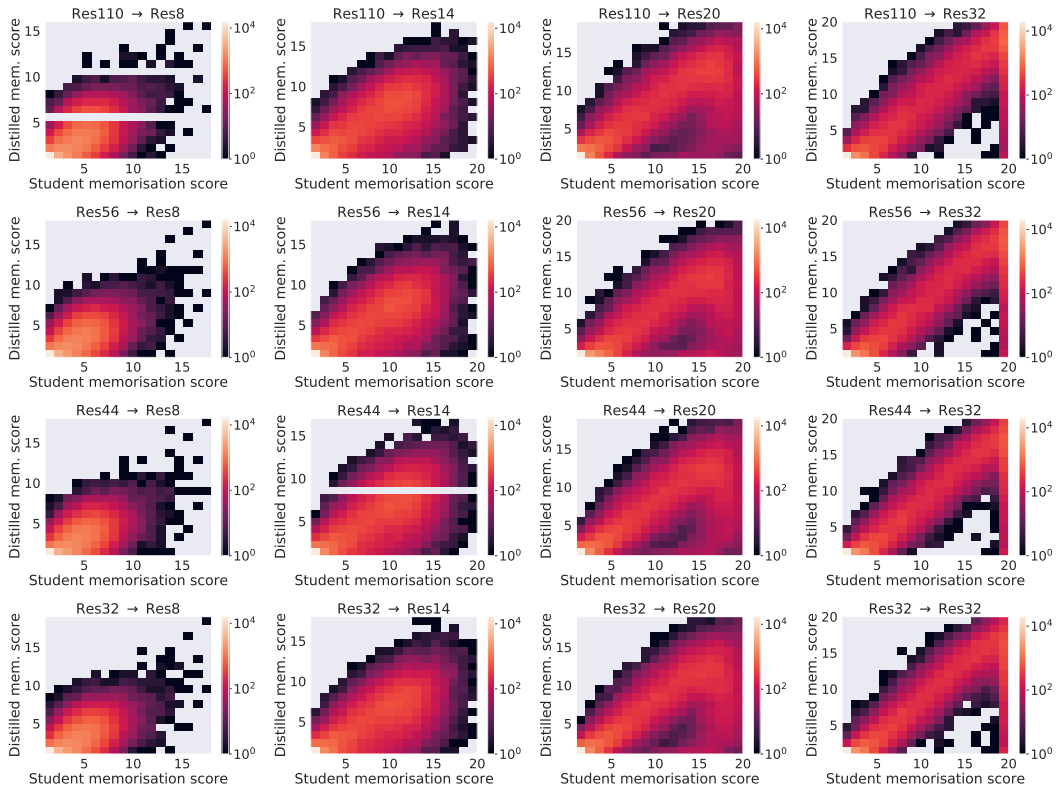


Figure 18: Contrasting per-example memorisation scores across distilled and one-hot student models for various teachers.

H.5 Memorisation trajectories on ImageNet

In Figures 21, 22, 23 we report per example memorisation trajectories for ImageNet with varying MobileNet architecture depths for selected labels: *toaster*, *tent* and *bubble* categories. We make similar observations to those made on CIFAR-100 trajectories. First, the *least changing* trajectories are the easiest examples, with consistently low memorisation across model sizes. Next, both the U-shaped and the decreasing trajectories are composed of harder examples. Finally, the most increasing

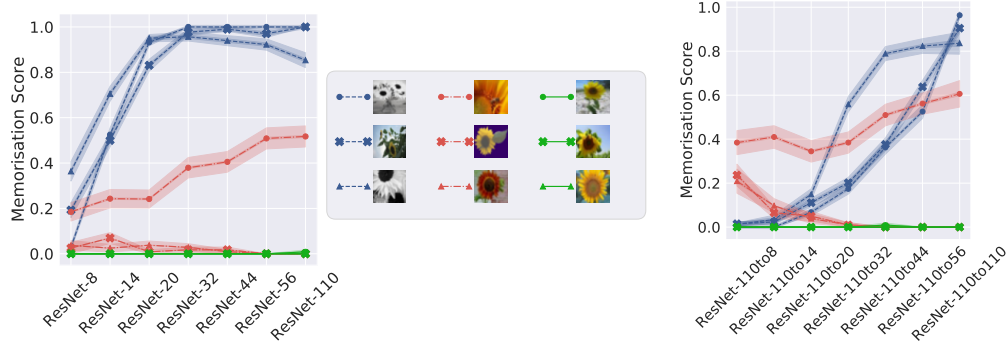


Figure 19: Evolution of memorisation score across one-hot (left) and distilled (right) models for examples across three groups: where memorisation is most *increased* by distillation (blue), most *decreased* by distillation (red), and where it *least changes* (green). We plot standard deviations of the Feldman score estimates around the example trajectories.

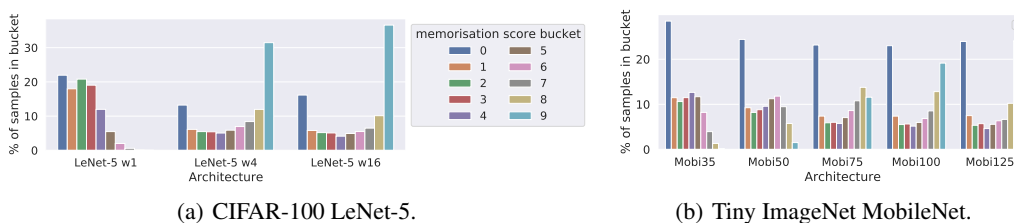


Figure 20: Distributions of memorisation scores across datasets and model architectures. We divide the range of memorisation scores into 10 equally-spaced memorisation score buckets. We consider LeNet-5 [49] models on CIFAR-100 training set and MobileNet models on Tiny Imagenet of varying sizes. We achieve multiple architecture versions for LeNet-5 by varying the widths: wk denotes a model where width is scaled k times compared to the original LeNet-5. We find an increasingly *bi-modal* distribution as the width increases.

trajectories are often more ambiguous or with an unclear label (e.g., the first example in the most increasing category for the *tent* label shows a dog), and some of the *bubble* examples don't seem to clearly show bubbles (e.g. the third most increasing example). Thus, we confirm that in the *most increasing* category, the examples can be mislabeled and ambiguous as for their label.

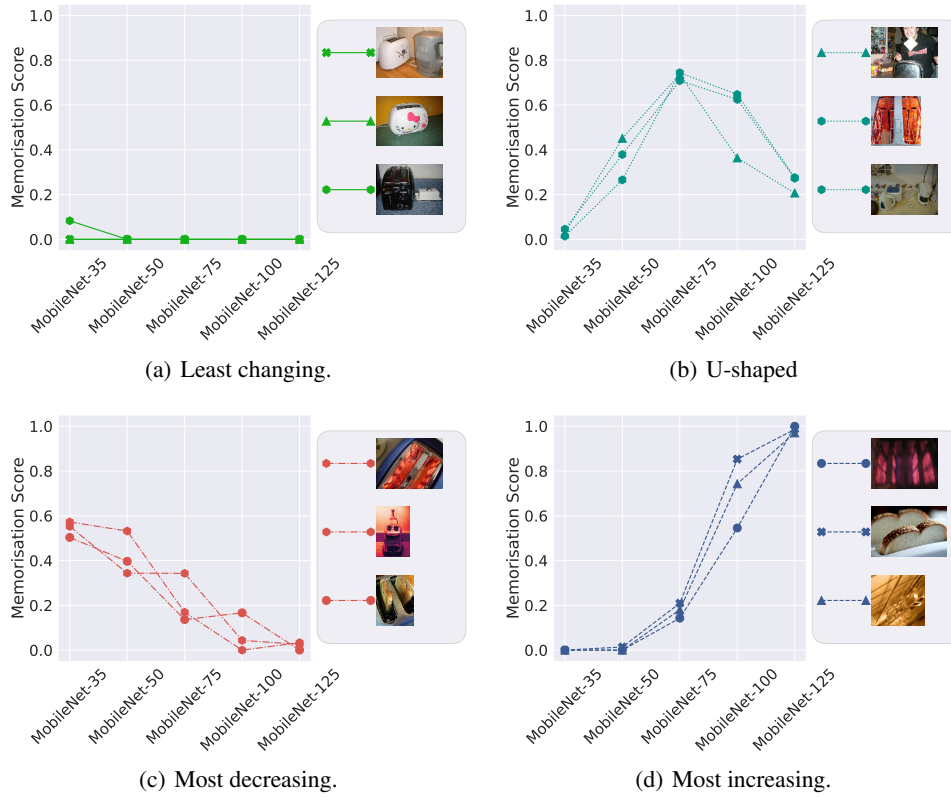


Figure 21: Per-example memorisation trajectories over depth for ImageNet examples from label *toaster*. We show that *training examples exhibit a diverse set of memorisation trajectories* across model depths: fixing attention on training examples belonging to the `sunflower` class, while many examples unsurprisingly have *fixed*, *decreasing* or *U-shaped* memorisation scores (*green*, *red* curves), *teal* curves), there are also examples with *increasing* memorisation *even after interpolation* (*blue* curves). Typically, easy and unambiguously labelled examples follow a *fixed* trend, noisy examples follow an *increasing* trend, while hard and ambiguously labelled examples follow either an *increasing*, *decreasing* or *U-shaped* trend; in §3.2 we discuss their characteristics in more detail.

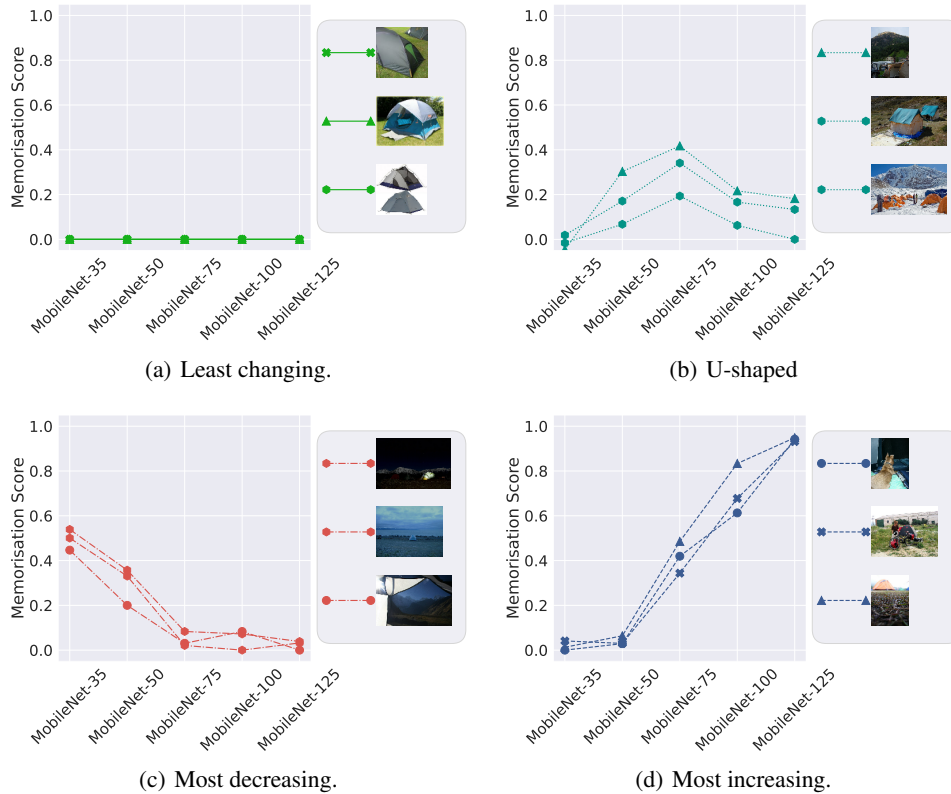


Figure 22: Per-example memorisation trajectories over depth for ImageNet examples from label *tent*. We show that *training examples exhibit a diverse set of memorisation trajectories* across model depths: fixing attention on training examples belonging to the `sunflower` class, while many examples unsurprisingly have *fixed*, *decreasing* or *U-shaped* memorisation scores (*green*, *red* curves), *teal* curves), there are also examples with *increasing* memorisation *even after interpolation* (*blue* curves). Typically, easy and unambiguously labelled examples follow a *fixed* trend, noisy examples follow an *increasing* trend, while hard and ambiguously labelled examples follow either an *increasing*, *decreasing* or *U-shaped* trend; in §3.2 we discuss their characteristics in more detail.

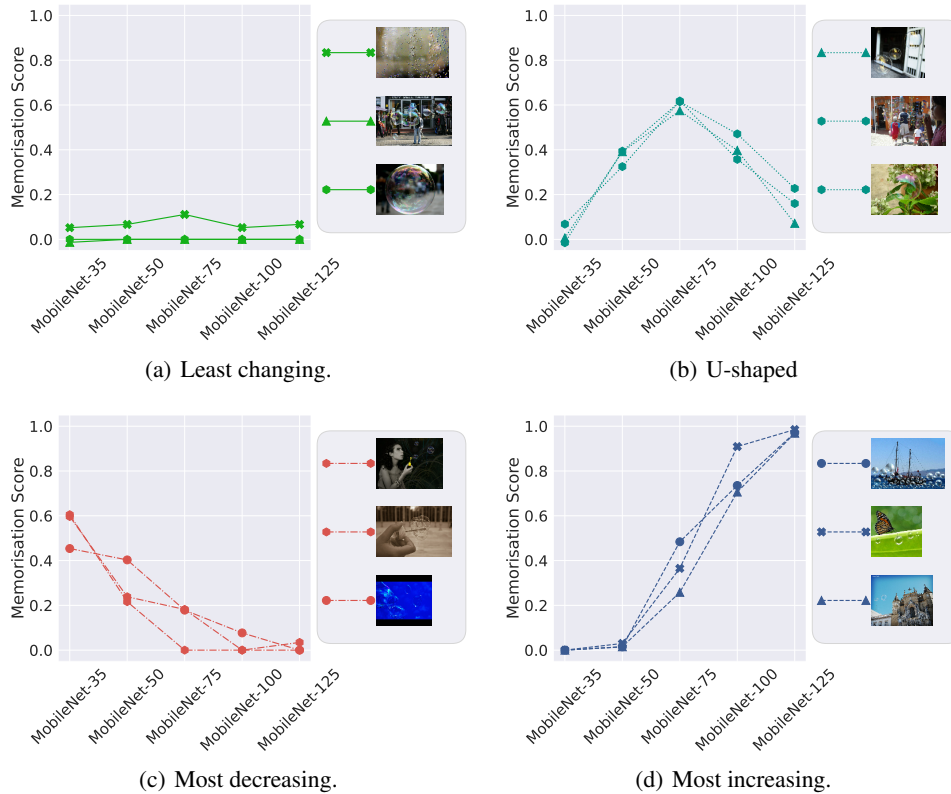


Figure 23: Per-example memorisation trajectories over depth for ImageNet examples from label *bubble*. We show that *training examples exhibit a diverse set of memorisation trajectories* across model depths: fixing attention on training examples belonging to the `sunflower` class, while many examples unsurprisingly have *fixed*, *decreasing* or *U-shaped* memorisation scores (*green*, *red* curves), *teal* curves), there are also examples with *increasing* memorisation *even after interpolation* (*blue* curves). Typically, easy and unambiguously labelled examples follow a *fixed* trend, noisy examples follow an *increasing* trend, while hard and ambiguously labelled examples follow either an *increasing*, *decreasing* or *U-shaped* trend; in §3.2 we discuss their characteristics in more detail.

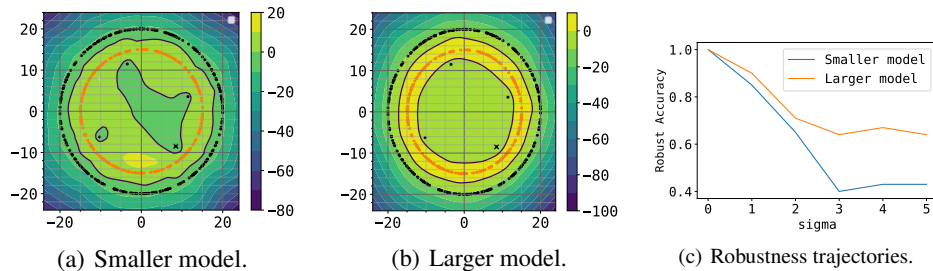


Figure 24: We show the learnt decision regions (i.e., the difference between the logits from the model assigned to the two classes) when training a smaller (1 hidden layer model with 10k dimensions) and a larger (3 hidden layers with 500 dimensions) models on an illustrative two-dimensional binary classification dataset. Note that unlike in Figure 13, here we *include* the highlighted outlier (denoted by the black cross). We observe how the larger model is more robust than the smaller model on the highlighted outlier, as denoted by the higher accuracy from the larger model on perturbed inputs with random Gaussian corruptions of varying standard deviations [25].

I Memorisation and robustness

Intriguingly, a distinct line of work studied the impact of capacity on *adversarial robustness*, e.g. Madry et al. [55] shows how model robustness increases with capacity. while Papernot et al. [64] showed how distillation can lead to improved adversarial robustness. It is thus natural to ask how adversarial robustness relates to memorisation. In order to measure the robustness difference between the two models from our example, we revisit the example discussed in Figure 13 and randomly perturb the highlighted outlier with random Gaussian corruptions of varying standard deviations and compare the accuracy on the perturbed example against the original label across the smaller and larger models [25]. We plot the decision regions of the compared models and the result of the robustness comparison in Figure 24, and find the larger model to be significantly more robust. That is intuitively expected, as denoted by the learnt decision regions being more smooth, and the inner circle being connected as opposed to the disconnected areas learnt by the small model.

To summarise, on the challenging example, we find the larger model to be more robust, while having lower memorisation.

J Additional experiments: prediction depth and cprox

The *prediction depth* has been shown to be closely related to the C-score [5]. Prediction depth computes model predictions at intermediate layers, and reports the earliest layer beyond which all predictions are consistent. These predictions were made using a k -NN classifier in Baldock et al. [5]. As demonstrated in Baldock et al. [5], prediction depth forms a lower bound on the stability-based memorisation score.

J.1 On the choice of probes for prediction depth

Baldock et al. [5] make a choice between k -NN and linear probes. In Appendix E, the authors notice how linear probes lead to all train examples having prediction depth equal to 0, leading to a trivial solution. Therefore, the authors settle on the k -NN probes, which don't provide a trivial solution even on the train set. However, the authors consider only three architectures, with the strongest model being ResNet-18, and the largest dataset CIFAR-100.

Our goal is to consider larger scale experiments from Baldock et al. [5] in terms of both the architectures and datasets, for which k -NN probes on large embeddings quickly become computationally prohibitive. In order to alleviate the computational complexity, we consider linear probes on embeddings after average pooling, leading to a non trivial distribution of score values across examples. One supporting argument for this approach is that in ResNet architecture, the embedding after the final layer is subjected to average pooling before passing to the classification layer. Thus, our approach to linear probes is consistent with how ResNet does classification.

In Figure 25, we show the comparison between k -NN and linear probes on average pooled embeddings. We see how there is a significant degree of similarity between the two distribution, except the low end of depths where the k -NN probes assign more examples. Notice how the distribution of score values for k -NN probes (leftmost figure) resembles that from [5] (see Figure 1 in [5]), despite the latter being computed on non-average pooled embeddings, contrary to the former.

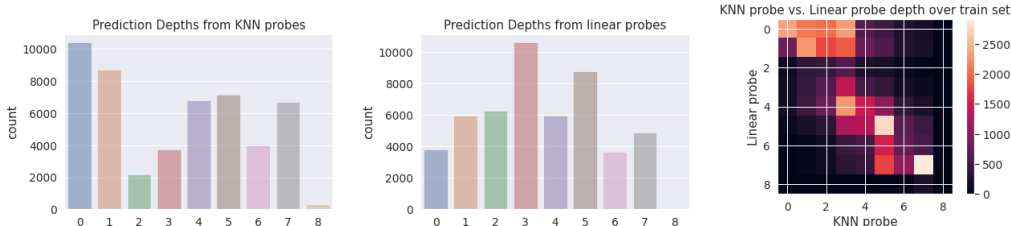


Figure 25: Prediction depth statistics on train examples from CIFAR-10 for ResNet-18 across linear or k -NN probes on average pooled embeddings after each layer. Notice how linear probes lead to fewer examples with prediction depth 0 compared to k -NN probes (two left-most figures). We notice how there is a high agreement between linear probes and k -NN probes (right-most figure), except where k -NN probes assign depth 0 or 1, where linear probes increase depth by up to 3, and in the medium range of depths, where linear probes increase the depth by up to 2.

J.2 Per-sample score trajectories

In Figure 26, we report additional results on how prediction depth and c-score proxy scores change per example across model depths. We confirm that the shift in score values is smaller than that for memorisation score (see Figure 8).

In Figure 27 we provide more details about the prediction depth score distributions. We see how across model architectures, the prediction depth and memorisation scores correlate to a large extent. At the same time, we see that the score marginal distributions are unimodal, contrasting with the bi-modal distributions we found for memorisation score.

In Figure 28, we plot trajectories of prediction depth over architecture depths for examples depicted in Figure 1. Recall that in the latter, we found a range of patterns depending on the relative change of memorisation score. For prediction depth, we find that the least changing in memorisation points get

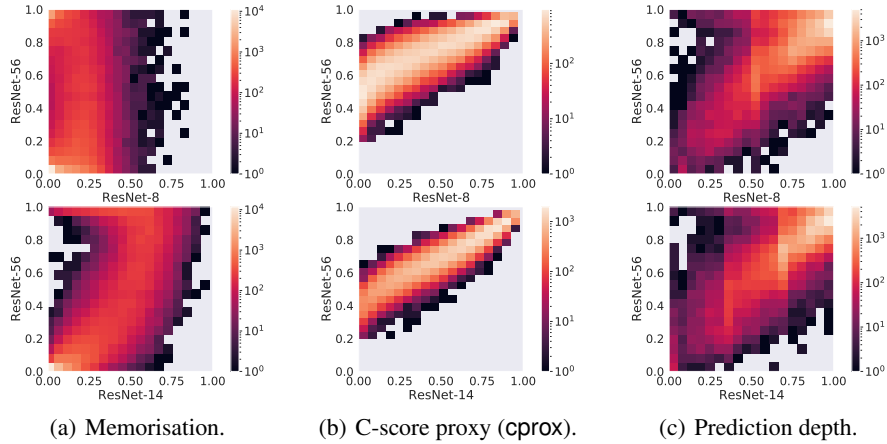


Figure 26: Contrasting per-example stability-based memorisation, prediction depth and `cprox` scores across architectures in different setups. Notice how `cprox` plot is concentrated around the diagonal to a greater extent than memorisation score. Prediction depth is also more concentrated around the diagonal, albeit to a lesser extent than `cprox` (notice there is more mass towards top left part of the heatmap for prediction depth than for `cprox`, but less than for memorisation score). Overall, the plots suggest that there are relatively few samples whose prediction depth or `cprox` score changes significantly with increased depth. By contrast, a non-negligible fraction of samples receive a low stability-based memorisation score under a ResNet-8 model, but a much higher score under a ResNet-56 model.

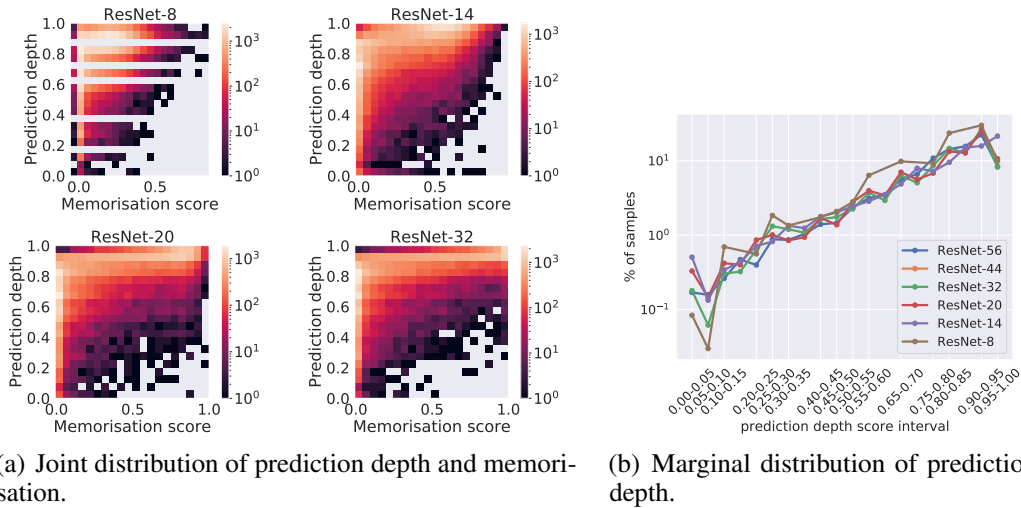


Figure 27: Relationship between stability-based memorisation (Equation 1) and prediction depth on CIFAR-100. The left plot shows a heatmap of the joint density under the two measures. There is a strong correlation with stability-based memorisation: the correlation to the memorisation score across examples is above 70% for all compared model depths. The right plot shows the marginal distribution of prediction depth over the CIFAR-100 training set across ResNet architectures. The marginals are unimodal, unlike the bi-modal distributions for stability-based memorisation scores.

the lowest depth across architectures, which may be interpreted as classifying them as the easiest. Interestingly, the most and the least changing examples in terms of their memorisation score are not clearly distinguished between when considering prediction depth: most of them get assigned a very high prediction depth scores across architectures.

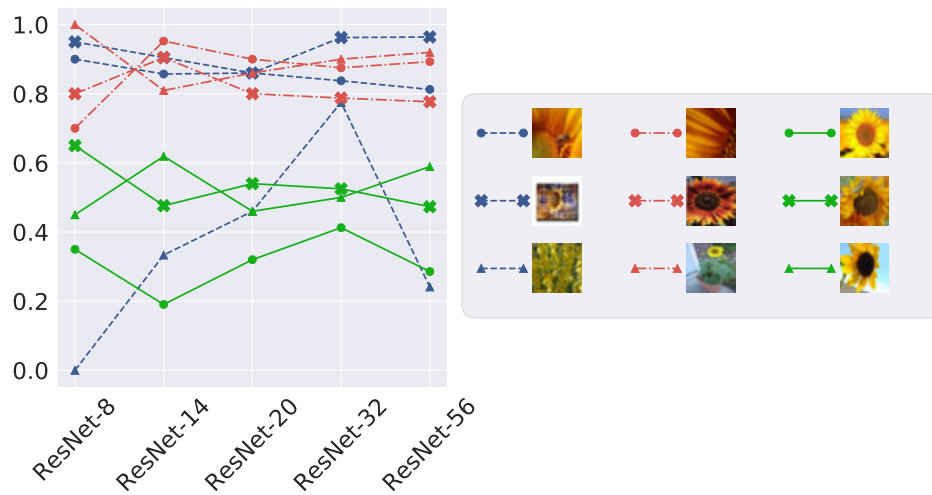


Figure 28: **Example Prediction Depth vs Model Size.** We report the normalized prediction depth score trajectories for the increasing, decreasing and not-changing memorisation examples from Figure 1. We find that examples become less changing in their score when considering prediction depth compared to memorisation score: their trajectory of score over architecture depths is usually roughly constant. This aligns with the heatmap in Figure 26 where we see that across various architecture depths the example prediction depth usually doesn't change much.